Integration of visual and antennal mechanosensory feedback during head stabilization in hawkmoths

Payel Chatterjee, Agnish Dev Prusty, Umesh Mohan, and Sanjay P. Sane*

National Centre for Biological Sciences,
Tata Institute of Fundamental Research,
Bangalore 560065,
India

*Corresponding Author: sane@ncbs.res.in

Key words:

Head stabilization, gaze stabilization, Johnston's organs, optic flow, *Daphnis nerii*

Highlights

1. Visual feedback contributes to head stabilization primarily during slower body rotation in hawkmoths.
2. Antennal mechanosensors contribute to head stabilization primarily during faster body roll.
3. Antennal mechanosensory feedback in head stabilization is mediated *via* Johnston's organ.
4. Restricting head movements affects flight control.

Summary

During flight maneuvers, insects exhibit compensatory head movements which are essential for stabilizing the visual field on their retina, reducing motion blur, and supporting visual self-motion estimation. In Diptera, such head movements are mediated *via* visual feedback from their compound eyes that detect retinal slip, as well as rapid mechanosensory feedback from their halteres - the modified hindwings that sense the angular rates of body rotations. Because non-Dipteran insects lack halteres, it is not known if mechanosensory feedback about body rotations plays any role in their head stabilization response. Diverse non-Dipteran insects are known to rely on visual and antennal mechanosensory feedback for flight control. In hawkmoths, for instance, reduction of antennal mechanosensory feedback severely compromises their ability to control flight. Similarly, when the head movements of freely-flying moths are restricted, their flight ability is also severely impaired. The role of compensatory head movements as well as multimodal feedback in insect flight raises an interesting question: in insects that lack halteres, what sensory cues are required for head stabilization? Here, we show that in the nocturnal hawkmoth *Daphnis nerii*, compensatory head movements are mediated by combined visual and antennal mechanosensory feedback. We subjected tethered moths to open-loop body roll rotations under different lighting conditions, and measured their ability to maintain head angle in the presence or absence of antennal mechanosensory feedback. Our study suggests that head stabilization in moths is mediated primarily by visual feedback during roll movements at lower frequencies, whereas antennal mechanosensory feedback is required when roll occurs at higher frequency. These findings are consistent with the hypothesis that control of head angle results from a multimodal feedback loop that integrates both visual and antennal mechanosensory feedback, *albeit* at different latencies. At adequate light levels, visual

feedback is sufficient for head stabilization. However, under dark conditions, antennal mechanosensory feedback is essential for the control of head movements.

INTRODUCTION

For the control of locomotor behaviors such as flight or walking, the ability to stabilize gaze is of central importance for reducing motion blur [1]. In diverse animals, gaze stabilization is achieved through sensorimotor circuits that rapidly sense and correct any deviation from the intended course, typically by eliciting reflexive motor responses of their head and body [1,2]. Of these, a class of responses called *optomotor reflexes* refer to those behaviors that occur in response to optic flow [3]. Although gaze stabilization typically requires eye as well as neck movements, in most flying animals including insects [1,2], birds [2,4] and bats [5], eye movements relative to the head are either reduced or absent. Such animals stabilize their gaze primarily using head and body movements guided by optomotor reflexes.

In insects, optomotor reflexes have mostly been studied in tethered flies (Diptera) using assays in which their heads were fixed to the thorax with glue while they were presented with a moving display [3]. In such preparations, the entire image stabilization is achieved through compensatory wing movements which may be tracked by infrared sensors or through high-speed videography [e.g.6]. The stroke amplitude difference between the wings can then be used to close the loop between display image and wing movement, allowing the fly to control the projection of the visual environment onto their eyes. This approach has been very successful in helping to uncover diverse visual capabilities of insects. However, because the head was glued to the thorax in these preparations, the role of head movements in image stabilization typically fell out of the purview of such studies. Recent work on the fruit flies *Drosophila melanogaster* suggests that head-fixation adversely affects mechanical power output for flight [7]. Moreover, head-fixation in tethered *Drosophila* impairs their ability to fixate on specific objects moving relative to ground; if an object is moving relative to a moving ground, wing movements depend on both object and ground motion, but head movements depend only on ground motion [8]. Head-fixation has also been shown to affect steering maneuvers in locusts *Locusta migratoria* [9]. Head and wing movements are thus crucial in steering maneuvers during flight and contribute strongly to gaze stabilization.

In Diptera, head stabilization is mediated by feedback from multiple sensory systems. These include visual feedback from their compound eyes and the mechanosensory feedback and/or feedforward control from their halteres which are modified hindwings that detect aerial rotations [10–12]. Additionally, mechanosensory proprioceptive structures in the ventral neck-prothorax region called prosternal organs also aid in head positioning [13,14]. The relative contributions of these sensory systems depend on the angular speed of the maneuver because vision typically provides feedback at slower rates than mechanosensors [10]. Importantly, during aerial maneuvers, haltere feedback combines non-linearly with visual feedback in some neck motor neurons to determine the compensatory head movements [15]. Thus, this system offers an interesting case study for how multisensory feedback from visual and mechanosensory modalities is integrated during locomotion. Because mechanosensory feedback from halteres is transduced at faster rates than visual feedback, it is hypothesized to play a key role in guiding wing movements during rapid maneuvers, whereas visual feedback mediates slower turns [16].

Fewer studies have focused on head stabilization in freely-flying insects as compared to tethered insects. Free-flight studies in diverse insects (honeybees *Apis mellifera* [17,18], blowflies *Calliphora vicina* [19]) show that rapid head turns precede sharp saccadic turns, whereas gaze stabilization between saccades ensures that the visual field largely translates over the retina, thereby enabling depth perception. When flying through a patterned, oscillating drum surrounding their nest entrance, freely flying bees adjust their head angle based on wide-field image movement in their visual field [17,18]. Moreover, visually induced head roll response is limited beyond specific roll frequencies, suggesting constraints to visually mediated gaze stabilization [17].

These studies demonstrate that optic flow plays a key role in head stabilization behaviour in both tethered and freely-flying insects. However, the role of mechanosensory feedback in gaze stabilization has been largely ignored in insects that lack halteres. Is head roll in these insects primarily visually-driven or does it also require mechanosensory feedback from some haltere analogue? Head stabilization in wasps appears to be primarily visually-mediated, although some degree of feedforward control has been suggested[36]. Similarly, in day-flying insects such as dragonflies, head stabilization appears to be dominated by visual feedback, and these insects contain adaptations that ensure passive inertial head stabilization [2,20,48]. Yet, being predatory insects, they achieve precise visual fixation of targets during prey capture during in flight prey capture [21,22]. The role of mechanosensory feedback in head movements in dragonflies remains an open question, especially as their antennae is very small and they do not possess halteres [23]. In contrast, nocturnal ants can stabilize their heads in darkness during walking suggesting mechanosensory input for stabilization [24]. However, the mechanosensors mediating head stabilization in non-Dipteran insects are yet to be identified.

One potential candidate for the mechanosensory mediation of head stabilization is the Johnston's organ, which is a highly sensitive mechanosensory structure situated in the antennal pedicel-flagellar joint of all insects [e.g.25,26]. The Johnston's organ consists of hundreds of concentrically arranged scolopidial units that are range-fractionated [27]. Antennal mechanosensors contribute in sensing airflow [28-30], and maintaining headwind orientation [31]. In moths, flight becomes unstable when the mechanosensory load on the Johnston's organ is reduced by clipping off their flagella [32,33]. In walking crickets, there is evidence that antennae contribute to compensatory head roll [34] and electrophysiological recordings from the neck motor system in flies further revealed that the ventral cervical nerve motor neuron in flies receive input from the antennae [35].

To determine the relative contributions of visual and mechanosensory inputs in gaze stabilization during flight, we studied head movements in the nocturnal hawkmoth, *Daphnis nerii*. In our experiments, moths were tethered to rotatable motor shafts, and we measured the compensatory counter-rotation of their head at two different angular rotations of their body under variable light conditions (Fig. 1A-F; see Materials and Methods). Additionally, we assessed their ability to use antennal mechanosensory feedback by ablating and reattaching their antennal flagellum. Our data show that at lower turning rates of the body, visual feedback is essential for head stabilization. However, at higher angular velocities, feedback from the Johnston's organs plays a crucial role in the control of head rotations, consistent with the hypothesis that this feedback combines with vision to modulate compensatory head movements. We also show that head movements are essential for controlled flight. Thus, the observed reduction in flight performance due to the loss of mechanosensory feedback from the antenna may be related to impaired gaze stabilization.

RESULTS

Head stabilization performance was characterized using three parameters: gain and phase of response, and compensation error which is a metric that combines both gain and phase. All three parameters must be considered to fully interpret a compensatory head response. When the gain is zero, the system offers no response and hence the phase values at this gain are uninterpretable. For non-zero gain, the phase values indicate how closely the response matches the stimulus in phase. However, in many cases, heavily delayed responses may appear as leading the stimulus in phase. Also, because gain and phase are inherently linked, they cannot be interpreted or statistically compared separately. The compensation error is a metric that enables us to statistically analyse these results.

Visual cues affect head stabilization at low frequency

To assess the role of visual cues in mediating compensatory head rotations, we provided rotating stimuli to tethered moths at different light levels (Twilight condition: ~250 lux; Dark condition: < 0.01 lux; see Materials and Methods). At each light level, the moths were rotated by ± 30 degrees about their longitudinal roll axis at oscillation frequencies of 2 Hz (Fig. 2A) and 6 Hz (Fig. 2B), while we measured their compensatory head movements.

Under twilight condition at 2 Hz, the compensation error was low with a median ± standard error of mean of 0.4 ± 0.02 (open circles, Fig. 2A, C). However, when we rotated the moths at 2 Hz under dark condition (filled circles, Fig. 2A, C, Supplementary Fig. 4 A, C), a reduction in gain (twilight condition median: 0.6, dark condition median: 0.4) and a shift in phase (twilight condition circular median: 177.6 °, dark condition circular median: 302.4 °, Supplementary Fig. 7 : Case 1 and 2) increased the compensation error to 1.2 ± 0.09, suggesting a severe reduction in their ability to generate compensatory head movements ($p = 0.0078$, Supplementary Table 3a, Supplementary Fig. 4 A, C). Additionally, the compensation error values of moths under dark conditions were more variable, which is also evident in the distribution of points in the polarscatter plots (compare open and filled circles, Fig. 2A; see also Fig. 2C, Supplementary Table 1). A different method of phase computation (see Methods) yielded a nearly identical result. (Supplementary Fig. 5 A, C, compensation error under twilight condition: 0.4 ± 0.02, dark condition: 1.2 ± 0.09, $p = 0.0078$, Wilcoxon signed-rank test). Thus, visual input plays a crucial role in mediating head stabilization at 2 Hz (Supplementary Movie-1).

We next increased the oscillation frequency to 6 Hz, and observed that under the twilight condition, the compensation error was 0.7 ± 0.02 (open circles, Fig. 2B-C). At 6 Hz, the phase-shift between the twilight and the dark condition was reduced in comparison to the 2 Hz case (twilight circular median:173.7 °, dark circular median: 214.2 °) whereas the gain between the two conditions was similar (Fig. 2B, Supplementary Fig. 4 B, D, see also Supplementary Fig. 7-Case 1 and 2). The compensation error (Fig. 2C) remained largely unaltered with a median ± standard error of mean of 0.7 ± 0.05 ($p = 0.5469$, Supplementary Table 3b). However, similar to the 2 Hz case, compensation error was more variable under dark conditions (compare open and filled circles, Fig. 2B, Supplementary Table 1). We got similar results using Fourier-based phase computation. (Supplementary Fig. 5 B, C, compensation error under twilight condition: 0.6 ± 0.02, dark condition: 0.7 ± 0.06, p =

0.4609, Wilcoxon signed-rank test). Thus, at 6 Hz, severe reduction of visual feedback did not greatly hamper head stabilization, suggesting that at roll rotation of higher frequency, an additional - perhaps mechanosensory - feedback played a role in head stabilization. However, the phase-shift and increased variability in the response in the dark condition suggests that some visual feedback may be required even at 6 Hz.

Antennal inputs affect head stabilization primarily at high frequency

Mechanosensory feedback from the antennae has been previously shown to mediate flight control in hawkmoths [32,33]. To test the hypothesis that it also plays a role in head stabilization, we clipped the antennal flagella, thus greatly reducing the inertial load of the antenna. We subjected these moths to roll stimuli (± 30º) at 2 Hz and 6 Hz in both twilight and dark conditions, and filmed the resulting head movements (Fig 3 A-E).

Under both twilight and dark conditions at 2Hz (Fig. 3E), the compensation error was significantly different between the *flagella-intact* (twilight: 0.4 ± 0.02; dark: 1.2± 0.09) and *flagella-clipped* groups (twilight: 0.5 ± 0.01; dark: 1 ± 0.01, p = 0.0107, p = 0.0133, Supplementary Table 3 c, d). Under the twilight condition, the gain values remained largely unaltered with a slight shift in phase in the *flagella-clipped* moths in comparison to the *flagella-intact* ones from a circular median of 177.6 ° to 174 ° (open circles, Fig. 2A, 3A, Supplementary Fig. 7 - Case 1 and 3). Under the dark condition, the gain was very low in *flagella-clipped* moths with a median of 0.1 (filled circles, Fig. 3A, Supplementary 4 E, G, Supplementary Fig. 7- Case 4). Because the gain values are very low, the phase values were uninterpretable in this context. Unlike in the *flagella-intact* group at 2 Hz under dark conditions, the variability of the compensation error was very low under *flagella-clipped* moths. (Fig. 3E, filled circles, Fig. 2A, 3A, Supplementary Table 1). The response (open and filled circles, Fig. 2A) of *flagella-intact* moths at 2 Hz in the dark could, therefore, potentially result from antennal mechanosensory input, in turn influencing compensatory head movements at the low frequency in the dark.

At 6 Hz (Fig. 3E), the compensation error was significantly different between the *control* (twilight: 0.7 ± 0.02, dark: 0.7 ± 0.05) and *flagella-clipped* (twilight: 0.8 ± 0.03, dark: 1.0 ± 0.03) groups in both twilight (p = 0.0064) and dark conditions (p = 0.0011) (Supplementary Table 3 e, f). Under twilight conditions, we observed a shift in phase in the *flagella-clipped* moths compared to the *flagella-intact* group from a circular median of 173.7 ° to 127.8 °

although the gains were similar (open circles, Fig. 2B, 3B, Supplementary Fig. 7-Case 1 and 3). Comparable to the responses observed at 2 Hz, the gain (median: 0.1, filled circles, Fig. 3B, Supplementary fig. 4H) and variability (Fig. 3E, Supplementary Table 1) were lowest in *flagella-clipped* moths under dark conditions. These observations suggest that at 6 Hz, antennal mechanosensory input may be critical for head stabilization. Despite reduced antennal mechanosensory feedback, there are some indications of head stabilization under twilight conditions (compare open circles to filled circles, Fig. 3B). This again suggests that visual feedback plays a role at this frequency. However, the compensation error of *flagella-clipped* moths under twilight condition at 6 Hz is significantly greater in comparison to 2 Hz ($p = 0.0156$, Wilcoxon signed-rank test) because there is a shift in phase from a circular median of 174 ° to 127.8 °. However, the gain values are similar (Supplementary Fig. 7, open circle: 3 A, B). Thus, the response due to visual feedback is reduced during faster body rolls.

Does restoring the mechanical load of flagella rescue head stabilization in the flagella-clipped moths? To determine this, we repeated the experiment in moths with reattached flagella. After reattachment of flagella, the head stabilization was similar to the performance of the moths with intact antennae, for all conditions. For both 2 Hz and 6 Hz rotations, the compensation error in *flagella-reattached* moths (Fig. 3C-E, Supplementary Fig. 4 I-L) was not significantly different from the *flagella-intact* group under twilight and dark conditions (see Supplementary Table 3 c-f for statistical comparisons). Similar to the response of the *flagella-intact* group at 2 Hz, we observed a phase-shift between the twilight and dark conditions in the *flagella-reattached* moths from a circular median of 177 ° to 297.6 ° at 2 Hz and from 149.4 ° to 216 ° at 6 Hz. (Supplementary Fig. 7-Case 5 and 6, Figs. 2 A, 3C). For 6 Hz rotations in the dark condition (Fig. 3E), the compensation error of the *flagella-reattached* moths differed significantly from the *flagella-clipped* group (Table 1f). The coherence estimates were also highly variable in *flagella-clipped* moths under the dark conditions in comparison to the corresponding *flagella-intact* and *flagella-reattached* groups (Supplementary Fig. 6A, Supplementary Table 2). Together, these experiments suggest that antennal mechanosensory input is required for head stabilization in hawkmoths primarily at higher frequency, besides some contribution at lower frequency as well (Supplementary Movie 2). Our results also indicate some contribution of visual feedback at higher frequency rotation.

The role of Johnston's organs in head stabilization

Johnston's organs respond to extremely subtle deformations and vibrations of the flagellum relative to pedicel [27]. Their role in flight stabilization has been highlighted in previous studies [32,33], and hence we specifically tested their contribution to head stabilization. In the experiments described above, the ability of the *flagella-clipped* moths to stabilize their heads was reduced although visual feedback may offset this effect to a certain extent at 2 Hz and to a lesser extent at 6 Hz. We therefore tested the hypothesis that this effect in moths with removed flagellar load was specifically due to the reduction of mechanosensory feedback from the Johnston's organs. To reduce feedback from the Johnston's organ, we glued the pedicel-flagellar joint of moths in which the Johnston's organ is embedded. Data from these experiments were compared with *sham-treated* moths in which the ~ 2nd-3rd annuli in the flagella were glued, rather than the pedicel-flagellar joint (Fig 4 A-E).

Under twilight and dark conditions for 2 Hz roll stimulus, the compensation error between the *sham* (twilight: 0.4 ± 0.02, dark: 1.2 ± 0.08) and *Johnston's organ glued* groups (twilight: 0.4 ± 0.01, dark: 1 ± 0.04) was not significantly different (Fig. 4E, $p = 0.5358$, $p = 0.0831$, Supplementary Table 3 g, h). However, similar to the *flagella-clipped* group, the *Johnston's organ glued* moths exhibited very low gain (median: 0.11) under dark conditions and therefore, their phase values in this condition are not interpretable (filled circles, Fig. 3A, 4C). Also, similar to the *flagella-intact* group, the *sham* group showed high variability in the dark conditions, and phase values shifted from 178.5° in twilight condition to 306.3° in dark condition (Supplementary Table 1, Fig. 4E, filled circles, 4A). At 6 Hz in both twilight and dark conditions, the compensation error differed significantly between the *sham* (twilight: 0.6 ± 0.03, dark: 0.6 ± 0.06) and *Johnston's organ glued* (twilight: 0.9 ± 0.05, dark: 1 ± 0.04) groups (Fig. 4E, $p = 0.0097$, $p = 0.0055$, Supplementary Table 3 i, j). Thus, we observed similar effects in *Johnston's organ glued* and *flagella-clipped* moths (Fig. 3A-B, E, 4C-E), suggesting that feedback from the Johnston's organ affects head stabilization. The coherence values were variable in the *Johnston's organ glued* group in comparison to those obtained in the *sham* group under dark conditions (Supplementary Table 2, Supplementary Fig. 6B).

Combinatorial effects of visual and antennal mechanosensory feedback

In the experiments presented here, maximal deviation in phase occurs when either visual feedback is reduced under dark conditions at low-frequency roll stimuli (compare Case 2 with the control Case 1; Supplementary Fig 7) or else when antennal mechanosensory feedback is reduced by clipping flagella or gluing JO a high-frequency roll stimuli (compare

Case 3 with Case 1; Supplementary Fig 7). When antennal feedback was restored by reattaching the flagellum, both gain and phase values were similar to the intact antenna case (e.g. compare Case 1 with Case 5, and Case 2 with Case 6; Supplementary Fig. 7). These data show that visual feedback is essential at low-frequency roll whereas antennal mechanosensory feedback is crucial at high-frequency roll maneuvers. If both visual and antennal mechanosensory feedback are reduced or eliminated, gain is reduced to zero or near zero values indicating that head roll response is absent (Supplementary Fig. 4 G, H), under which conditions, the phase values are uninterpretable. On the other hand, when *flagella-intact, flagella-reattached* and *sham* moths (Fig. 2, 3, 4) underwent low-frequency roll in dark conditions, the compensation error exceeded 1 and the gain was non-zero, indicating that the head response was elicited but in the wrong direction due to the phase-shift from the ideal stabilization scenario (filled circles in Figs. 2A, 3C, 4A). In the corresponding *flagella-clipped* and *JO-glued* moths, the gain values were very low indicating that no response was elicited (filled circles; Fig. 3A, 4C) in absence of antennal mechanosensory feedback, resulting in compensation error values near 1 (Fig. 3E, 4E).

Restricted head movements cause loss of flight performance in freely flying moths

Together, the above experiments on tethered moths indicated that mechanosensory feedback from the antennal Johnston’s organ is involved in head stabilization, in addition to the visual feedback from its retina (Fig 5). We next hypothesized that flight impairment observed in previous studies in the flagella-clipped hawkmoths, *Manduca sexta* (Sane et al, 2007) may arise from inability of these hawkmoths to stabilize their head during flight. If that is the case, then we expect moths with restricted heads to show similar flight impairments as those observed in the *flagella-clipped* moths. We filmed the free-flight trajectories (see Methods) of moths whose head-movements were restricted. We compared these with *control* moths in which the head was free to move, and with *sham* moths which underwent the same procedure as experimental moths but without head restriction. In our experiments, out of 12 animals in each group, 11 *control* animals, 12 *sham*-treated and 8 experimental *head-restricted* moths produced free flight behavior (comparison with internal control: Supplementary Fig. 1A, B). The flight duration of *control* (73 ± 17.0 s) and *sham* (34 ± 9.3 s) groups were significantly longer compared to the moths with restricted head-motion (1.5 ± 0.7 s) (Fig. 6A, p = 0.0001, Supplementary Table 3k). We also observed a difference in the flight behavior of the *head-restricted* moths in comparison to the *control* and *sham* moths. Whereas the *control* and *sham* moths took off smoothly and pitched up to a considerable height, the *head-restricted* moths were unable to pitch up, and consequently stayed close to the ground usually touching it, and became unstable as soon as they became airborne (Supplementary Movie-3). The frequency of these moths (1 ± 0.1 per second) colliding with the walls of flight chamber was significantly greater than in *control* (0.4 ± 0.05 per second) and *sham* (0.3 ± 0.05 per second) moths, thus indicating impairment in their flight performance (Fig. 6B, p = 0.0002, Supplementary Table 1l).

In the free-flight assay described above, the moths were not presented with any specific stimuli to generate flight activity. Thus the flight duration depended entirely on when the moth voluntarily chose to stop flapping and land on a surface, which caused substantial variability in the free flight data on control moths. In the head-restricted moths however, flight duration is significantly lower compared to all other cases (Supplementary Fig. 1B), implying that *head-restricted* moths cannot fly in a controlled manner and collide more frequently per unit time, when compared to moths in the *control* and *sham* group.

DISCUSSION

Compensatory head movements are crucial for stability in free flight (Fig. 6 A-B). The data presented in this paper show that such compensatory head roll in tethered flight is mediated *via* a combination of visual and antennal mechanosensory feedback in the hawkmoth, *Daphnis nerii* (Fig. 5).

Role of visual feedback in flight and gaze control in hawkmoths

In diurnal insects, visual feedback plays a key role in eliciting compensatory head movements during complex maneuvers [10,36]. However, at lower light levels, the visual system transduces at slower rates thereby imposing severe constraints on insects, especially during aerial manuevers[37]. Previous studies on freely flying hawkmoths have documented the role of visual feedback in flower tracking by quantifying their responses at different light intensities (diurnal hawkmoths, *Macroglossum stellatarum* [33,38], crepuscular/nocturnal hawkmoths, *Manduca sexta* [38,39] and *Deilephila elpenor* [38]).). Electrophysiological studies from the wide-field motion-sensitive neurons of nocturnal hawkmoths suggest spatial and temporal tuning of their neurons to their ecological niche [40]. Together, these studies show that despite the handicap of slow visual transduction rates, hawkmoths can fly or perform aerial maneuvers under low light levels.

We conducted this study on the Oleander hawkmoth *Daphnis nerii* primarily because it typically flies in low light and we used similar light levels as used in the flower tracking studies of crepuscular and nocturnal hawkmoths *Manduca* and *Dielephila* (300 Lux and 0.3 Lux [38,39]). Our data show that gaze stabilization in *Daphnis nerii* requires visual feedback at low temporal frequency, and antennal mechanosensory feedback at higher temporal frequencies at which purely visual means of gaze stabilization may be constrained due to the requirement for both spatial and temporal pooling of photons to form images or derive motion information. Specifically, we hypothesize that gaze stabilization is enhanced by a fast response *via* the antennal mechanosensory feedback loop which ensures that the head remains sufficiently stable to enable temporal and spatial integration of photons by the superposition eyes. Our study design opted for a 3D distribution of objects rather than a 2D display, and hence does not allow us to delineate visual and mechanosensory stimuli. However, because each experiment is specifically compared with its corresponding control scenario, the results described here would hold for any arbitrary 3D visual scene. In general, the cross-modal feedback between visual and haltere systems in flies [15,41] or between visual feedback and antennal position in hawkmoths [42] means that it is difficult to completely isolate visual and mechanosensory feedback even in experiments that employ a 2D open-loop display.

Role of antennal mechanosensory feedback in control of head stabilization and flight

We used two treatments to reduce the antennal mechanosensory feedback from the Johnston's organs. In one case, we clipped off flagella to cause mechanical unloading of Johnston's organ and in the second case, we glued the pedicel-flagellar joint. In both cases, we observed similar impairment of head stabilization (Fig. 3E, 4C). Moreover, regluing the flagella and thus restoring Johnston's organ feedback caused recovery of head stabilization. These results suggest that Johnston's organ is the key antennal mechanosensory organ involved in head stabilization. In these experiments, *flagella-clipped* moths were more strongly affected than the *JO glued* moths, indicating some residual feedback from Johnston's organ feedback after gluing the pedicel-flagellar joint but not enough to ensure proper head stabilization (Fig. 4).

Although previous experiments have indicated that antennal mechanosensory feedback is crucial for maintaining stable flight [32,33], the precise link between antennal mechanosensors and flight has remained largely unexplored. Antennae sense airflow in diverse insects [25], and moths and bees modulate antennal positioning during flight [28,29]. Antennae help in maintaining headwind orientation [31], mediating abdominal flexion [43], and flight balance [32,33]. In this study, we show that Johnston's organ feedback affects compensatory head roll. Moreover, restriction of head movement causes impediment in flight performance. Thus, flight impairment due to loss or reduction of Johnston's organ input may result in part from their inability to control compensatory head movements.

Head stabilization in tethered hawkmoths is under-compensated

In our experiments, the gains for compensatory head movements ranged from 0.2 - 0.6 depending on the frequency of the forced body rotations under twilight condition, which meant that the head was not fully stabilized in its horizontal orientation. We ruled out the hypothesis that such low gain results from the stimulus amplitude exceeding anatomical constraints of the moth's neck motor system limiting the angular range of head roll rotations, as the gain was less than 1 also for low-amplitude stimuli (Supplementary Fig. 3). Previous studies in diverse insects including flies [44], locusts [45], and wasps [36] show that head stabilization does not fully compensate for the imposed stimulus. Undercompensated head stabilization for low stimulus amplitudes has also been previously observed in blowflies [44], suggesting that compensatory head rotations are only one of several components contributing to optomotor reflexes and are not the only mechanism involved in maintaining a level gaze. In free-flight, perhaps, both compensatory head rotations and body rotations would contribute to a level gaze. It remains to be seen if such under-compensation exists in freely flying conditions and has a clear function in flying insects. Alternatively, gaze stabilization in insects may be inherently undercompensated, as insects have been reported to not respond to a stable pattern (detailed discussion in [44]).

Multisensory control of reflexes

A key result of these experiments is that, just as flies integrate haltere and visual feedback for head stabilization [2,10,12], the head stabilization reflex in moths also requires the integration of visual and antennal mechanosensory inputs. In absence of a detailed frequency analysis, we were unable to determine if the combinatorial effect of visual and antennal mechanosensory is linear or non-linear. A consistent result across these studies is that visual feedback influences head stabilization behaviour in a lower frequency regime, whereas mechanosensory feedback – whether from antenna or halteres – influences head stability at a higher frequency regime. In flies, halteres detect fast angular velocities of thorax rotation and elicit head stabilization with a gain of 0.1 around 50 °/s, which reaches a maximum of about 0.75 at around 1000 °/s [10,16]. Similarly, in moths the antennal mechanosensory feedback affects tracking only at high frequencies (> 2Hz) of flower oscillations, whereas visual feedback is key at lower frequencies [33]. Indeed, the frequency range in which visual and antennal inputs influence head stabilization in the present study is similar to the frequency range reported in studies on freely flying moths [33]. In flies, some neck motor neurons require simultaneous activation of halteres and visual pathways for elicting spikes, thus setting up a gating mechanism which would enable compensatory head movements in a dynamic range that is in between the maximum sensitivities of the motion vision and haltere system [15, also see 40]. Whereas head wind and visual stimuli together elicit spikes in the Ventral Cervical Nerve Motorneuron (VCNM) of the neck motor system, they do not individually fire action potentials in VCNM in the blowfly, *Calliphora vicinia.* In that study, the removal of the arista of the antenna abolished this VCNM response [35]. Thus, flies may also possess a similar gating mechanism in the visual and antennal pathways that acts at the level of neck motor neurons. It is likely that similar gating exists in the visual and antennal mechanosensory pathways in non-Dipteran insects.

Conclusion

Our experiments demonstrate that head stabilization in hawkmoths requires the combined feedback from the compound eyes and antennal mechanosensors. Under sufficient lighting and during slower turns, hawkmoths are able to stabilize their head using visual feedback. However, under dark conditions or during faster turns, the role of antennal mechanosensory feedback from the Johnston’s organs is also essential. In absence of gaze stabilization, flight control in freely flying hawkmoths is severely impaired. Taken together, these results show that the loss of flight control due to reduction of antennal mechanosensory feedback may result at least partly from an inability to stabilize gaze. Thus, our results point to the importance of visual and mechanosensory integration in head stabilization behaviour of insects. In Diptera, this has been shown to involve mechanosensory feedback from halteres in addition to the neck proprioceptive feedback from prosternal organs and other potential contributions from mechanosensory feedback in legs, wings and abdomen. The data presented here show that for non-Dipteran insects such as hawkmoths, mechanosensory feedback is derived partly from the antennal Johnston’s organs.

Acknowledgements

We thank M. Kemparaju and Allan Francis Joy for maintaining the moth culture, Shivansh Dave for his help with setting up the stepper motor, free-flight arena set-up, camera synchronization and free-flight pilot experiments, and the mechanical and electronics workshops at NCBS for help with the apparatus. Funding for this study was provided by grants from Air Force Office of Scientific Research (AFOSR) # FA2386-11-1-4057 & # FA9550-16-1-0155, & National Centre for Biological Sciences (Tata Institute of Fundamental Research) to SPS. We acknowledge support of the Department of Atomic Energy, Government of India, under project no. 12-R&D-TFR-5.04-0800 and NCBS core computational facilities, supported under 12-R&D-TFR-5.04-0900.

Author contributions

Study design: S.P.S, U.M, P.C, A.D.P, Methodology: U.M, P.C, A.D.P, Experiments and analysis: P.C, A.D.P, Manuscript preparation: P.C, A.D.P, U.M., S.P.S

Declaration of interests

The authors declare no competing interests

Figure Legends

Figure 1. Methods and representation of experiments. (A) A schematic of the experimental set-up illustrating the relative positions of the stepper motor, tethered moth and camera. (**B**) Front view of the moth with lines drawn through the digitized points and the angles used for analysis. θ_{thorax} is the angle between the tether position and the vertical and $\theta_{\mathrm{head\text{-}thorax}}$ represents angle between head and thorax. **(C)** Traces representing ideal head stabilization ($\theta_{\mathrm{head\text{-}thorax}}$: yellow) and no head stabilization ($\theta_{\mathrm{head\text{-}thorax}}$: cyan) in response to an imposed roll stimulus of amplitude ± 30 deg and frequency of 2 Hz (θ_{thorax}: black). **(D)** Representative experimental trial showing head roll rotations that do not fully compensate the forced body rotations in moths (violet trace, $\theta_{\mathrm{head\text{-}thorax}}$). **(E)** Polar plot representing gain and phase of the different conditions in (C) and (D). Each point represents gain in the radial axis and phase in the circular axis. The points are colour-coded with reference to the plots in (C) and (D). Compensation error (labelled ε in the figure, also see Supplementary methods) is the distance between a representative point (purple) and the ideal head stabilization (yellow). The case of zero gain (blue) indicates the absence of any response. (F) A cluster of points belonging to a sample treatment is enclosed by a 95% confidence ellipse and the mean of the points is highlighted in red.

Figure 2. **Visual feedback mediates head stabilization. (A, B)** Polarscatter plots (with 95% confidence ellipses) of head roll response to body roll frequency of 2 Hz **(A)** and 6 Hz **(B)** in control moths. In each plot, the twilight condition is marked by open circles, the dark condition is marked by filled circles and their mean is highlighted in red. **(C)** Box plots comparing compensation error between twilight and dark (filled boxplots) trials at 2 Hz (left two boxplots) and 6 Hz (right two boxplots). The data-points are scattered on the plots. Points representing the same animal in twilight and dark trials are connected with lines. Also see Supplementary Figs. 4, 5, Supplementary Movie_1.

Figure 3. Antennal feedback is required for head stabilization. (A-D) Polarscatter plots (with 95% confidence ellipses) of 2 Hz **(A, C)** and 6 Hz **(B, D)** roll frequencies in *flagella-clipped* **(A, B)** and *flagella-reattached* moths **(C, D)**. In each plot, the twilight condition is marked by open circles, the dark condition is marked by filled circles and the mean is highlighted in red. **(E)** Boxplots comparing compensation error between *control* (C), *Flagella-clipped* (FC) and *Flagella-reattached* (FR) moths for twilight and dark (filled boxplots) trials at 2 Hz (left six boxplots) and 6 Hz (right six boxplots). Note that the control dataset in this plot is used from the previous experiment (Fig. 2C). Also see Supplementary Fig. 4, Supplementary Movie_ 2

Figure 4. Johnston's organ contributes to head stabilization (A-D) Polarscatter plots (with 95% confidence ellipses) of 2 Hz (A, C) and 6 Hz (B, D) roll frequencies in *sham* (A, B), and *Johnston's organ glued* (C, D) moths. In each plot, the twilight condition is marked by open circles, the dark condition is marked by filled circles and the mean is highlighted in red. **(E)** Boxplots comparing compensation error between *sham* and *Johnston's organ glued* (JO glued) moths for twilight and dark trials at 2 Hz (left four boxplots) and 6 Hz (right four boxplots).

Figure 5. Summary Figure A block diagram illustrating the role of visual and antennal mechanosensory feedback in the head stabilization response. The visual and antennal mechanosensory feedback sections of the loop have time delays (τ_v , τ_m) which vary based on illumination levels and flagella ablation state respectively. These responses combine to elicit the head roll response.

Figure 6. **Restricting head movements impairs flight stability.** Boxplots comparing flight bout duration **(A)** and collision frequency **(B)** between control, sham and head-restricted moths in free-flight. Also see Supplementary Figs. 1, 2, Supplementary Movie_3

Supplementary Movie_1. **Role of visual feedback in head stabilization.** Representative videos of *flagella-intact* moths under twilight and dark conditions at 2 Hz.

Supplementary Movie_2. **Role of antennal feedback in head stabilization.** Representative videos of *flagella-intact and flagella-clipped* moths under dark conditions at 6 Hz.

Supplementary Movie_3. Role of head movements in free-flight behaviour of hawkmoths. Representative videos of *control*, *sham* and *head-restricted* moths showing stable flight, side-wall collision, unstable flight, sliding and skidding locomotion.

METHODS

Resource availability

Lead contact

Further information and requests for resources and reagents should be directed to and will be fulfilled by the Lead Contact, Prof. Sanjay P. Sane (sane@ncbs.res.in)

Materials availability

This study did not generate new unique reagents.

Data and code availability

The datasheets and codes are deposited in Mendeley data and available in the following link:

https://data.mendeley.com/datasets/2trxj9gwsw/draft?a=89356c26-e581-40c6-935d-c1d4a0401074

Any additional information required to reanalyze the data reported in this paper is available from the lead contact upon request.

Experimental model and subject details

Moth breeding

We used adult ~1 day post-eclosion *Daphnis nerii* bred in a greenhouse for experiments. The temperature of the greenhouse was maintained at ~28°C. The adult male and female moths were released in a netted chamber in the greenhouse for mating and egg-laying. Larvae of all instars were reared on a natural diet of *Nerium oleander* leaves inside mesh-topped boxes in the greenhouse. The pupae were initially kept in sawdust inside the mesh-topped boxes after which they were transferred to a netted cage to allow emergence. Adult *Daphnis nerii* begin flying around sunset and remain active through the night (Operating light levels: ~ 0.05-250 Lux, unpublished observations)

Experiments on tethered moths

In this assay, we measured the ability of moths to generate compensatory head movements in response to externally imposed body rotations, under conditions of variable illumination (to manipulate visual feedback) and in presence or severe reduction of antennal flagella (to manipulate antennal mechanosensory feedback).

Method details

Treatment procedure

We anesthetized moths by keeping them in -20°C for about 8 minutes. The thorax of each moth was descaled before attaching to it a 3 mm neodymium magnet using cyanoacrylate glue. There were 5 experimental groups: *control*, *flagella-clipped*, *flagella-reattached*, *Johnston's organ glued* and its corresponding *sham* procedure.

The *control* group was anaesthetized and tethered just as the experimental groups, but underwent no further treatment. In the *flagella-clipped* moths, we cut both the left and right flagella around the 3rd-4th annuli thereby reducing the mechanical load on the Johnston's organs. In the *flagella-reattached* moths, we cut and then reattached the excised flagella to their stumps using cyanoacrylate glue. Finally, for the *Johnston's organ glued* group and its corresponding *sham* treatment, we kept the moths on a metal-plate placed atop an ice-bath throughout the treatment procedure (~30 min). In both groups, the head and the base of the antennae were descaled to expose the pedicel-flagellar joint. Cyanoacrylate glue was applied to the pedicel-flagellar joint in the *Johnston's organ glued* group. In the sham group, glue was applied approximately at the junction between 2nd-3rd annulus of the flagellum. This ensured that the gluing procedure itself did not affect head stabilization. All the groups were given about half an hour of recovery post treatment before starting the experimental assay.

Behavioral Protocol

We mounted the moths on a tether which was attached to the shaft of a stepper motor (NEMA 23, 1.8° step angle, 10.1 kg.cm torque). The tether was bent into a U-shape to ensure that the longitudinal axis of the moth aligned with the shaft axis (Fig. 1A). To achieve smooth motion, we used a low-noise microstepping driver (Leadshine ND556) with a 125 microstep resolution (i.e. 25000 steps/revolution) in all our experiments. Using a microcontroller board (PJRC Teensy 3.5, 120 MHz), we generated stimuli of desired frequencies. We used split magnets for tethering the moths and at the end of the tether rod. In this procedure, neodymium magnets were split and the two half-magnets were joined to prevent slipping of the magnets about the yaw axis. The tether was rotated with a sinusoidal stimulus of peak-to-peak amplitude of 60 degrees (± 30 degrees) and the moth head was aligned with the shaft of the motor to ensure that the roll stimulus was around the longitudinal axis going through the head, approximately aligned with the pivot point of the neck motor system. We ensured that the moths were actively flapping their wings during the experiments.

We placed a high-speed camera (V.611, Phantom) frontally and filmed the moths at 1200 frames/second using 200 μs exposure. We painted the clypeus and labrum of the moth head with black acrylic color (Fig.1B), put small white papers on it and the tether rod for easy digitization. IR LEDs were mounted around the lens for additional lighting. All the groups were filmed in two ambient light conditions under which the moths are typically active (*Twilight*: ~250 lux; *Dark*: < 0.01 lux). We used a lux meter (Center 337; Range: 0.01 - 40000 lux) to measure light intensity around the moth. We rotated the tether at two frequencies: 2 Hz (low) and 6 Hz (high) for 8 cycles each, corresponding to mean angular velocities of 240°/s (low) and 720°/s (high) respectively. The maximum stimulus frequency our stepper motor could reliably generate was 6 Hz. Frequencies of 2 Hz and 6 Hz are in alignment with the dynamic range of stimuli provided in previous studies of flower tracking in other hawkmoth species. In the diurnal hawkmoth, *Macroglossum stellatarum* [33], antennal mechanosensory feedback was reported to play a significant role in flower tracking in the frequency range of 2-5 Hz. Further, under similar light levels used in our study, flower tracking was affected between the light levels in another study in the crepuscular hawkmoth, *Manduca sexta*, approximately in the frequency range of 2-8 Hz[39]. At the beginning and end of each stimulus period, a quarter of the sinusoidal oscillation of the tether movement was replaced with a linear ramp to avoid excessive accelerations and thus, potential shifts of the magnetic tether. The corresponding time periods of the responses were excluded from our analysis. The sequence of the light conditions and the roll frequencies tested was randomized across all moths.

Quantification and statistical analysis

Analysis

The videos were digitized using a custom C++ program in OpenCV library. We then calculated the angles between the thorax and frame vertical (θ_{thorax}) and between head and frame vertical (θ_{head}) in MATLAB. From the above angles, we computed the angle between the thorax and head ($\theta_{\text{head-thorax}}$) (Fig. 1B). The raw data were filtered using a 7th order low-pass Butterworth filter with cut-off frequency of 25 Hz, to eliminate the wing-beat induced noise in the head movements which occurs at the wingbeat frequency of *Daphnis nerii* (~ 30 Hz). The average amplitude at 2 Hz and 6 Hz was calculated by Fourier transform from the corresponding time series. We calculated the gain using the formula:

$$\text{Gain} = \frac{\text{Average amplitude of } \theta_{\text{head}-\text{thorax}}}{\text{Average amplitude of } \theta_{\text{thorax}}} \qquad (1)$$

The phase-difference (hereafter referred to as phase) between θ_{thorax} and $\theta_{\text{head-thorax}}$ was computed by cross-correlating the two time-series in MATLAB. The time difference corresponding to the maximum correlation between the two time-series was used for estimating phase. Phase (in radians) was computed from time difference using the equation:

$$\text{Phase} = 2\pi * (\text{frequency of oscillation}) * (\text{time difference}) \qquad (2)$$

We also estimated the phase-difference in *flagella-intact* moths based on a Fast Fourier Transformation of the responses in MATLAB [46] (Supplementary Fig. 5), where the complex output of FFT contains both magnitude and phase at each frequency.

If the animal stabilizes its head perfectly (i.e. fully compensated head stabilization), the gain is 1 and the phase is 180° (Fig. 1C). When the animal does not stabilize its head, the gain is 0 (Fig. 1C). If the gain is <1, then head stabilization is under-compensated (Fig. 1D). We represent gain and phase using polar scatter plots in which gain is represented in the radial axis and phase is depicted by the direction of each dot in the circular axis (Fig. 1E). A cluster of points, representing the results obtained during a particular treatment, is enclosed by a 95% confidence ellipse [47] (Fig. 1F). Head-compensation error parameter ε was computed as the distance between the perfect head stabilization point and the experimental point from a trial (Fig. 1E; for details see supplementary information). In this representation, the compensation error (ε) can range from 0 to 2 with an ε of 0 representing perfect head stabilization and corresponds to ($r = 1$, $\theta = 180^{\circ}$) in the polar-scatter plots (Fig. 1E). The point corresponding to ($r = 1$, $\theta = 0^{\circ}$) assumes an ε of 2 and as the error increases from 0 to 2, there is a reduction in the compensatory head roll. In the point corresponding to ($r = 0$, $\theta = 0^{o}$), there is no head movement relative to the thorax and therefore, no compensation.

We have also computed the magnitude-squared coherence between the stimulus and response time domain signals in all the groups at the stimulus frequencies in MATLAB (Supplementary fig. 6). Magnitude squared coherence is a function of power spectral densities of stimulus, response and their cross power spectral density, assuming values range from 0-1. A value of 1 indicates that the stimulus and response time domain signals are well-matched at that frequency.

Statistical tests

Because the data were not normally distributed, we used non-parametric tests to statistically compare the head-compensation error between the different treatment groups in all cases. As the light and dark trials were conducted on the same animal (in Fig 2C), we used a paired Wilcoxon's signed-rank test to compare the data. We compared the *control*, *flagella-clipped* and *flagella-reattached* groups using a Kruskal-Wallis test as the groups were independent. To further identify which groups were statistically different, the Kruskal-Wallis test was followed by a post-hoc comparison with a Nemenyi test. The unpaired data (in Fig. 4C) were compared using a Wilcoxon ranksum test, a non-parametric test used for statistically comparing two independent groups.

Free-flight assay

To address whether restriction of head movements in moths impact their free-flight performance, we conducted the following experiments.

Method details

Moths were divided into three groups including *control*, *sham* and *head-restricted* moths. Initially, all the groups were cold-anesthetized by placing them in -20°C for approximately 8-12 minutes. *Control* moths did not undergo any head restriction treatment, but went through the same anesthesia procedures as the other two groups. In the experimental *head-restricted* group, we partially removed the scales in the dorsal neck-prothorax region using a paintbrush and put tiny drops of molten dental wax at the neck using a heated wire. The wax solidified to make a bridge between prothorax and the posterior head, restraining any relative motion between head and thorax. In the *sham* group, we partially descaled the dorsal neck-prothorax region and put a similar amount of molten wax on another part of the prothorax, thus allowing the head to freely move relative to the thorax. All the moths were allowed to recover for one hour after the treatment.

The hawkmoths were next released inside a transparent acrylic flight chamber (1 m X 1 m X 0.8 m; Supplementary Fig. 2A) and their flight performance were observed and filmed both before (as internal control) and after treatment for each of the *control*, *sham* and *head-restricted* groups. These experiments were conducted in a large greenhouse in the evening around dusk during their naturally active periods. Before the experiments commenced, moths with obvious flight defects were discarded. Moths with no obvious flight defects underwent the three treatment conditions and their flight performance was filmed. Two tripod-mounted monochrome cameras (Pointgrey BFS-U3-13Y3M) were placed orthogonally and synced together to film the behavior simultaneously through transparent walls of the flight chamber (Supplementary Fig. 2A). A low-power bulb (Philips Deco Yellow 15 watts) hung approximately 15 cm above the ceiling of the flight chamber provided nearly uniform, low-intensity illumination inside the arena. The light intensity, as measured by a light meter (Center 337; Range: 0.01 to 40000 lux), was ~1.56 lux at the center of the arena's base, the area around which the moth was released. The moth was stimulated with air-puff to initiate flight. The behavior was filmed at a resolution of 1280 X 1024 pixels at 30 frames per second with an exposure time of 33 ms.

In a separate batch of moths, we tested the efficacy of the wax treatment by restricting the insect head movements using the previously described tethered assay for roll stabilization (Fig. 1A). Using this assay, we ascertained that head movements relative to the thorax were completely abolished in moths with waxed neck joints (Supplementary Fig. 2B-D).

Quantification and statistical analysis

Analysis

The duration of a flight bout was defined as the time spent between post-warmup take-off and termination of wing flapping upon landing. The take-off time was noted when the legs left the ground whereas the landing time was noted when the moth finally touched down and ceased flapping its wings. In some cases, the partially airborne moth skidded on the ground or crawled with forelegs touching the side walls even while the wings were flapping at high amplitude (Supplementary Movie 3). These moths were not considered flying as long as their legs touched the ground, and thus time spent in any intermediate skidding and crawling was subtracted from the total duration of a flight bout. Collisions with the side walls were observed and noted. Skidding and crawling were not considered as collisions except the initial contact with the wall. Collision frequency was calculated as the total number of collisions with any side wall divided by the flight bout duration.

Statistical analysis

Because the groups were unpaired and did not have a Gaussian distribution, we statistically compared flight bout duration and collision frequency between the *control*, *sham* and *head-restricted* moths using a non-parametric Kruskal-Wallis test, followed by a post-hoc Nemenyi test (Fig. 6). As the before and after treatments within each of *control*, *sham* and *head-restricted* groups were conducted on the same animal (in Supplementary Fig 1A, B), we used a paired Wilcoxon's signed-rank test to compare the data.

References

1. Land, M.F. (1999). Motion and vision: Why animals move their eyes. J. Comp. Physiol. - A Sensory, Neural, Behav. Physiol. *185*, 341–352.
2. Hardcastle, B.J., and Krapp, H.G. (2016). Evolution of Biological Image Stabilization. Curr. Biol. *26*, R1010–R1021.
3. Borst, A. (2014). Fly visual course control: Behaviour, algorithms and circuits. Nat. Rev. Neurosci. *15*, 590–599.
4. Necker, R. (2007). Head-bobbing of walking birds. J. Comp. Physiol. A Neuroethol. Sensory, Neural, Behav. Physiol. *193*, 1177–1183.
5. Eitan, O., Kosa, G., and Yovel, Y. (2019). Sensory gaze stabilization in echolocating bats. Proc. R. Soc. B Biol. Sci. *286*.
6. Duistermars, B.J., Reiser, M.B., Zhu, Y., and Frye, M.A. (2007). Dynamic properties of large-field and small-field optomotor flight responses in *Drosophila*. J. Comp. Physiol. A Neuroethol. Sensory, Neural, Behav. Physiol. *193*, 787–799.
7. Cellini, B., and Mongeau, J.M. (2020). Active vision shapes and coordinates flight motor responses in flies. Proc. Natl. Acad. Sci. U. S. A. *117*, 23085–23095.

8. Fox, J.L., and Frye, M.A. (2014). Figure-ground discrimination behavior in Drosophila. II. Visual influences on head movement behavior. J. Exp. Biol. *217*, 570–579.
9. Rowell, C.H.F., and Robert, D. (1992). Locust flight steering. J. Comp. Physiol. A, *171*, 41-51
10. Hengstenberg, R. (1993). Multisensory control in insect oculomotor systems. 285–298.
11. Hengstenberg, R. (1988). Mechanosensory control of compensatory head roll during flight in the blowfly *Calliphora erythrocephala* Meig . J. Comp. Physiol. A, 151–165.
12. Schwyn, D.A., Heras, F.J.H., Bolliger, G., Parsons, M.M., Krapp, H.G., and Tanaka, R.J. (2011). Interplay between feedback and feedforward control in fly gaze stabilization (IFAC).
13. Preuss, T., and Hengstenberg, R. (1992). Structure and kinematics of the prosternal organs and their influence on head position in the blowfly *Calliphora erythrocephala* Meig. J. Comp. Physiol. A, *171*, 483–493.
14. Paulk, A., and Gilbert, C. (2006). Proprioceptive encoding of head position in the black soldier fly, *Hermetia illucens* (L.) (Stratiomyidae). J. Exp. Biol. *209*, 3913–3924.
15. Huston, S.J., and Krapp, H.G. (2009). Nonlinear Integration of Visual and Haltere Inputs in Fly Neck Motor Neurons. J. Neuroscience, *29*, 13097–13105.
16. Sherman, A., Dickinson, M.H. (2003). A comparison of visual and haltere-mediated equilibrium reflexes in the fruit fly *Drosophila melanogaster*. J. Exp. Biol. *206*, 295–302
17. Boeddeker, N., and Hemmi, J.M. (2010). Visual gaze control during peering flight manoeuvres in honeybees. Proc. R. Soc. B. 277, 1209–1217.
18. Wehner, R., and Flatt, I. (1977). Visual Fixation in Freely Flying Bees. Zeitschrift fur Naturforsch. - Sect. C J. Biosci. *32*, 469–472.
19. Van Hateren, J.H., and Schilstra, C. (1999). Blowfly flight and optic flow. J. Exp. Biol. *1500*, 1491–1500.
20. Gorb, S.N. (1999). Evolution of the dragonfly head-arresting system. Proc. R. Soc. Lond. B. *266*, 525-535.
21. Olberg, R.M., Seaman, R.C., Coats, M.I., and Henry, A.F. (2007). Eye movements and target fixation during dragonfly prey-interception flights. J. Comp. Physiol. A Neuroethol. Sensory, Neural, Behav. Physiol. *193*, 685–693.
22. Lin, H.T., and Leonardo, A. (2017). Heuristic Rules Underlying Dragonfly Prey

Selection and Interception. Curr. Biol. *27*, 1124–1137.

23. Gewecke, M., Heinzel, H.., and Philippen, J. (1974). Role of antennae of the dragonfly Orthetrum cancellatum in flight control. Nature *249*, 584–585.
24. Raderschall, C.A., Narendra, A., and Zeil, J. (2016). Head roll stabilisation in the nocturnal bull ant *Myrmecia pyriformis* : implications for visual navigation. J. Exp. Biol. 219, 1449–1457.
25. Gewecke, M. (1974). The Antennae of Insects as Air-Current Sense Organs and their Relationship to the Control of Flight. Exp. Anal. Insect Behav., 100–113.
26. Sant, H.H., and Sane, S.P. (2018). The mechanosensory-motor apparatus of antennae in the Oleander hawk moth (*Daphnis nerii*, Lepidoptera). J. Comp. Neurol. *526*, 2215–2230.
27. Dieudonné, A., Daniel, T.L., and Sane, S.P. (2014). Encoding properties of the mechanosensory neurons in the Johnston's organ of the hawk moth, *Manduca sexta*. J. Exp. Biol. *217*, 3045–3056.
28. Khurana, T.R., and Sane, S.P. (2016). Airflow and optic flow mediate antennal positioning in flying honeybees. Elife *5*, *e14449*, 1–20.
29. Natesan, D., Saxena, N., Ekeberg, Ö., and Sane, S.P. (2019). Tuneable reflexes control antennal positioning in flying hawkmoths. Nat. Commun. *10*, 1–15.
30. Taylor, G.K., and Krapp, H.G. (2007). Sensory Systems and Flight Stability: What do Insects Measure and Why? Adv. Insect Physiol. *34*
31. Fuller, S.B., Straw, A.D., Peek, M.Y., Murray, R.M., and Dickinson, M.H. (2014). Flying *Drosophila* stabilize their vision-based velocity controller by sensing wind with their antennae. Proc. Natl. Acad. Sci. *111*, E1182–E1191.
32. Sane, S.P., Dieudonné, A., Willis, M.A., and Daniel, T.L. (2007). Antennal mechanosensors mediate flight control in moths. Science. *315*, 863–866.
33. Dahake, A.,Stockl, A.L.,Foster, J.J., Sane, S.P., Kelber, A. (2018) The roles of vision and antennal mechanoreception in hawkmoth flight control. Elife *7*, *e37606*, 1–21.
34. Horn, E., and Bischof, H. (1983). Gravity Reception in Crickets : The Influence of Cereal and Antennal Afferences on the Head Position. J. Comp. Physiol. 150, 93–98.
35. Haag, J., Wertz, A., and Borst, A. (2010). Central gating of fly optomotor response. PNAS *2010*.
36. Viollet, S., and Zeil, J. (2013). Feed-forward and visual feedback control of head roll orientation in wasps (*Polistes humilis*, vespidae, hymenoptera). J. Exp. Biol. *216*, 1280–1291.

37. Warrant, E., and Dacke, M. (2011). Vision and Visual Navigation in Nocturnal Insects. Annu. Rev. Entomol. *56*, 239–254.

38. Stöckl, A.L., Kihlström, K., Chandler, S., and Sponberg, S. (2017). Comparative system identification of flower tracking performance in three hawkmoth species reveals adaptations for dim light vision. Philos. Trans. R. Soc. B Biol. Sci. *372*.

39. Sponberg, S., Dyhr, J.P., Hall, R.W., and Daniel, T.L. Luminance-dependent visual processing enables moth flight in low light. Science *348*, 1245–1249.

40. Theobald, J.C., Warrant, E.J., and O'Carroll, D.C. (2010). Wide-field motion tuning in nocturnal hawkmoths. Proc. R. Soc. B Biol. Sci. *277*, 853–860.

41. Mureli, S., Thanigaivelan, I., Schaffer, M.L., and Fox, J.L. (2017). Cross-modal influence of mechanosensory input on gaze responses to visual motion in *Drosophila*. J. Exp. Biol. *220*, 2218–2227.

42. Krishnan, A., and Sane, S.P. (2014). Visual feedback influences antennal positioning in flying hawk moths. J. Exp. Biol. *217*, 908–917.

43. Hinterwirth, A.J., and Daniel, T.L. (2010). Antennae in the hawkmoth *Manduca sexta* (Lepidoptera , Sphingidae) mediate abdominal flexion in response to mechanical stimuli. J Comp Physiol A. *196*, 947–956.

44. Hengstenberg, R., Sandeman, D., and Hengstenberg, B. (1986). Compensatory head roll in the blowfly Calliphora during flight. Proc. R. Soc. B Biol. Sci. *227*, 455-482

45. Hensler, K., and Robert, D. (1990). Compensatory head rolling during corrective flight steering in locusts. J. Comp. Physiol. A, *166*, 685–693.

46. Hristo Zhivomirov (2021). Phase Difference Measurement with Matlab, MATLAB Central File Exchange, Mathworks

47. Wang, B., Shi, W., and Miao, Z. (2015). Confidence analysis of standard deviational ellipse and its extension into higher dimensional Euclidean space. PLoS One *10*, 1–17.

48. H. Mittelstaedt (1950). Physiologie des Gleichgewichtsinnes bei fliegenden Libellen Z. Vergl. Physiol., *32*, 422-463

Chatterjee, Prusty, Mohan, Sane
Figure 1

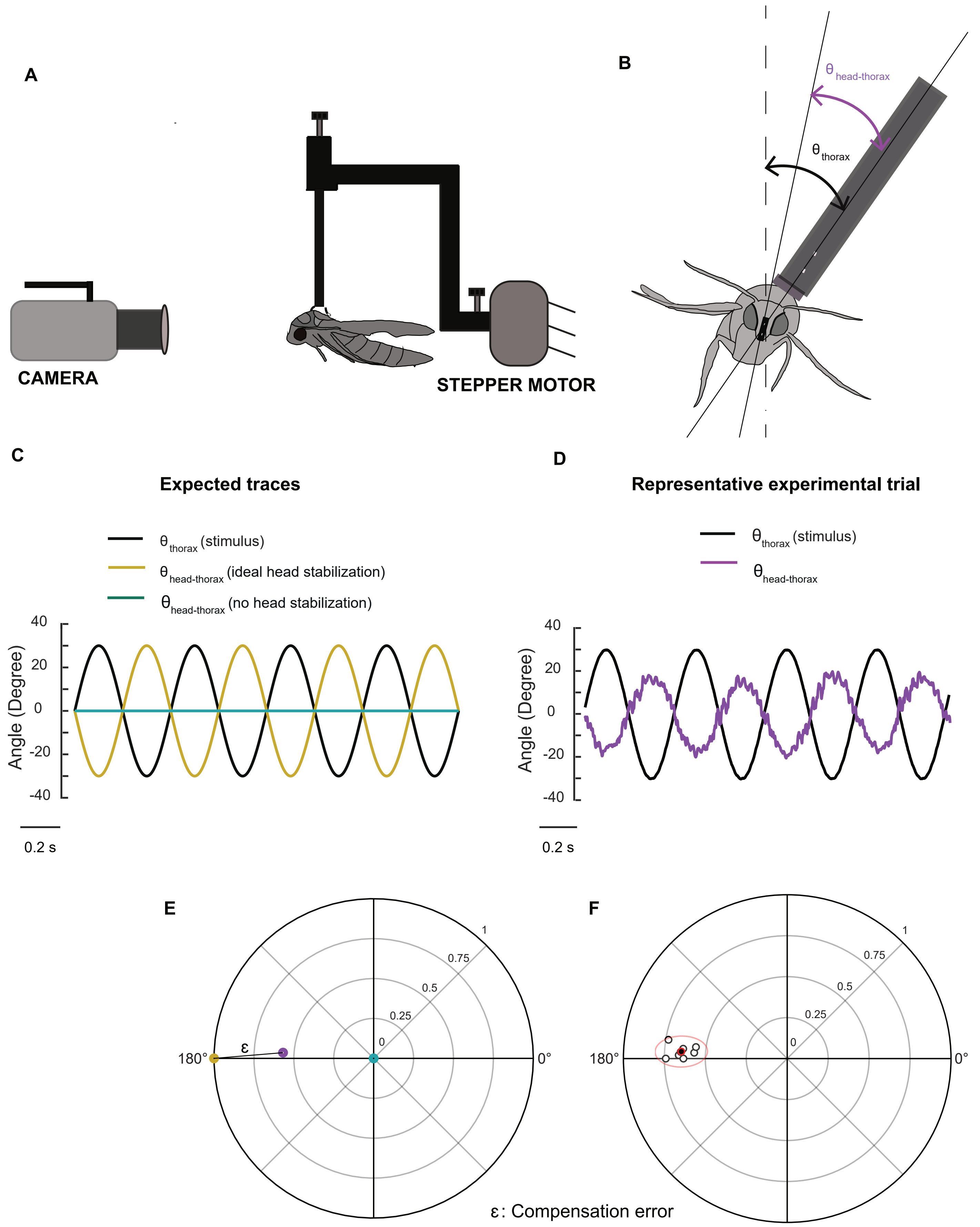

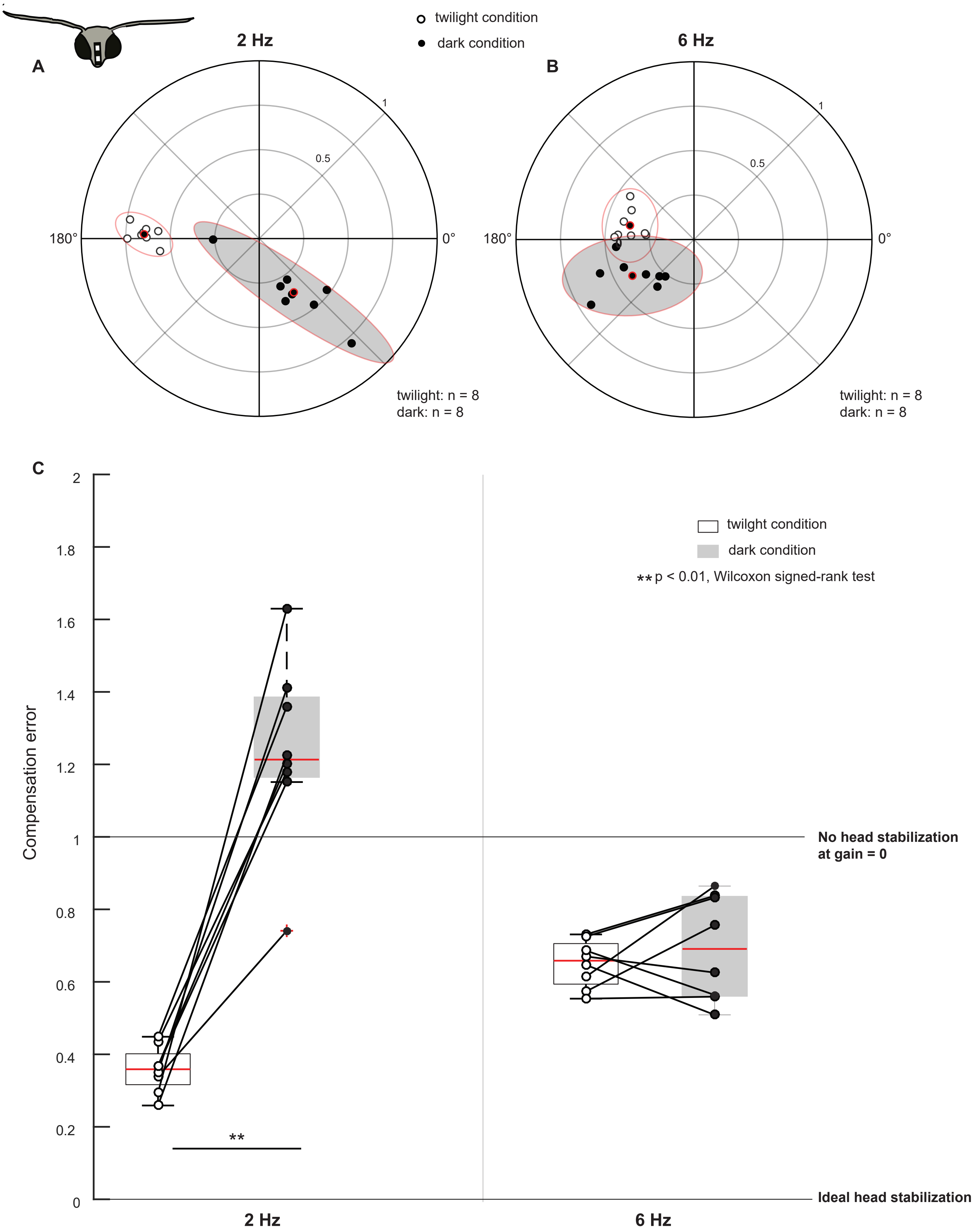
A
2 Hz
twilight condition
dark condition
6 Hz
B
1
0.5
180°
0°
1
0.5
180°
0°
twilight: n = 8
dark: n = 8
twilight: n = 8
dark: n = 8
C
Compensation error
2
1.8
1.6
1.4
1.2
1
0.8
0.6
0.4
0.2
0
twilght condition
dark condition
** p < 0.01, Wilcoxon signed-rank test
No head stabilization
at gain = 0
**
Ideal head stabilization
2 Hz
6 Hz

Chatterjee, Prusty, Mohan, Sane
Figure 3

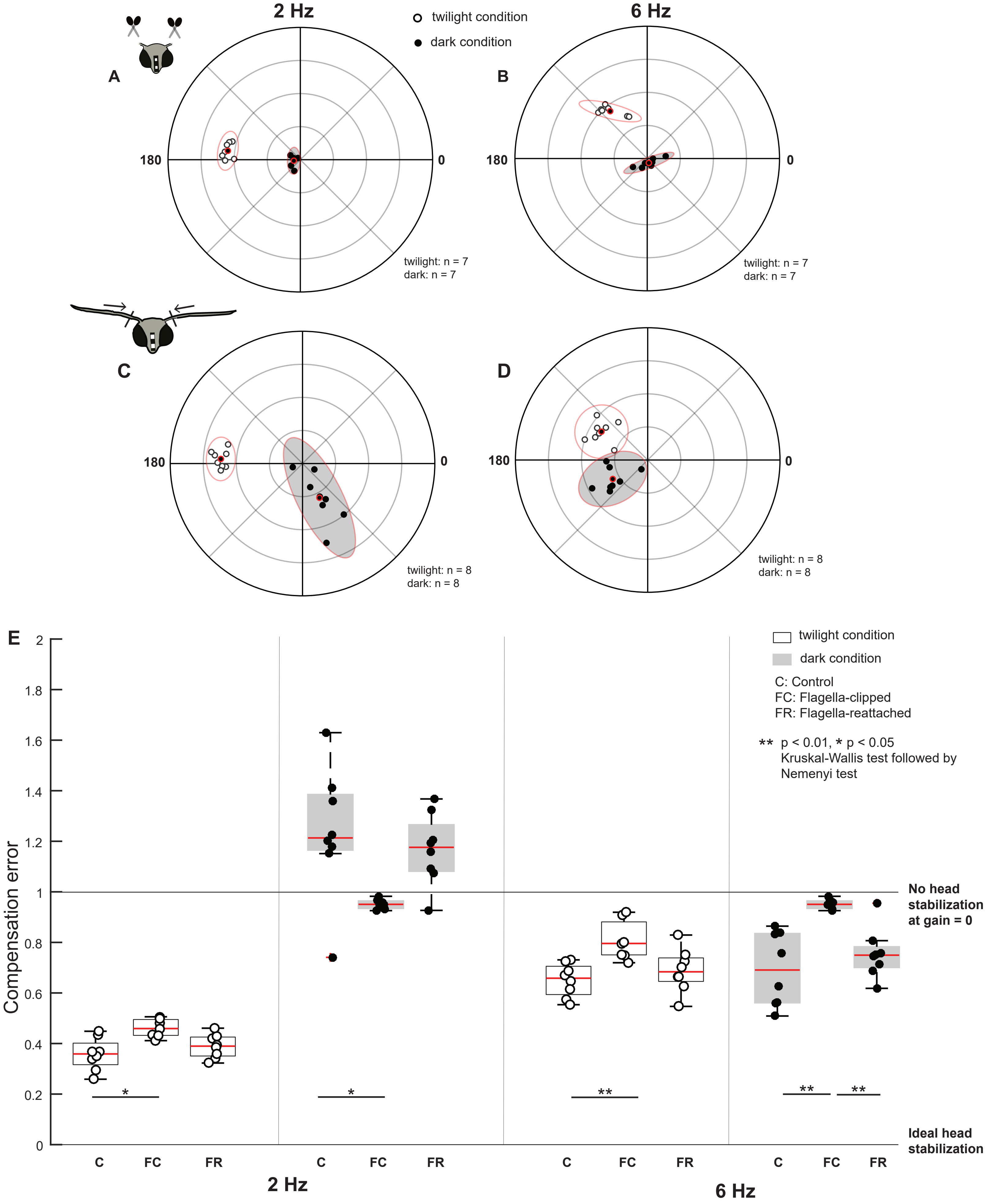

Chatterjee, Prusty, Mohan, Sane
Figure 4

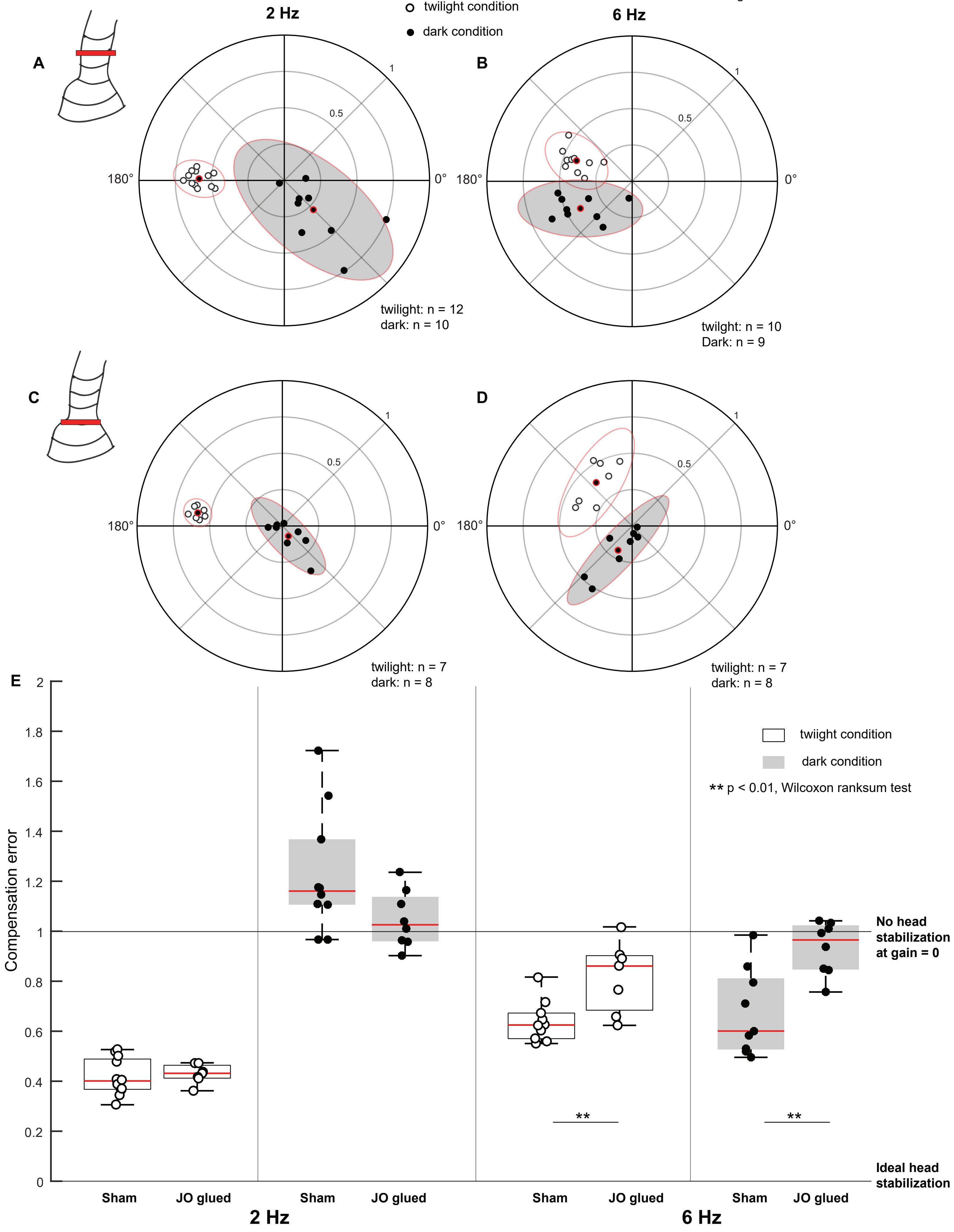

A

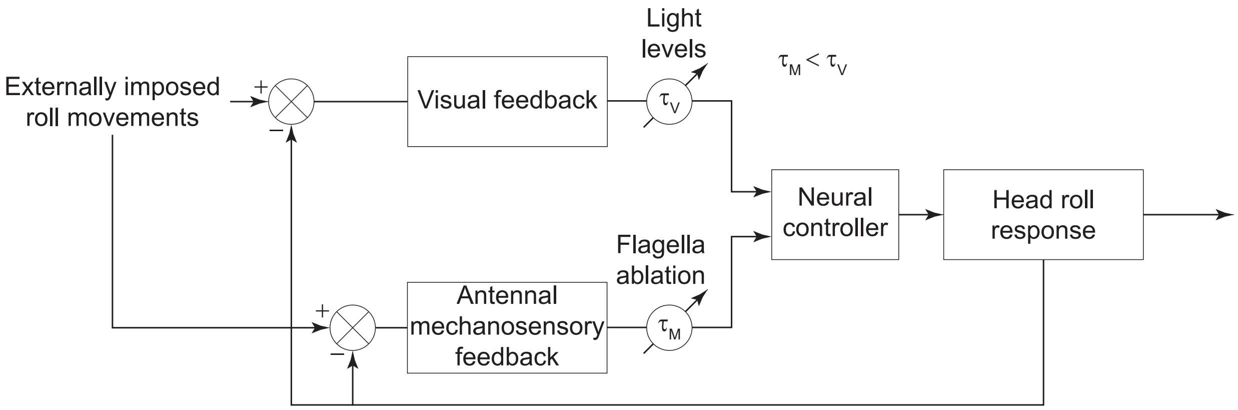
Externally imposed roll movements
+
−
Visual feedback
Light levels
τ_V
$\tau_M < \tau_V$
Neural controller
Head roll response
Flagella ablation
+
−
Antennal mechanosensory feedback
τ_M

Figure 6

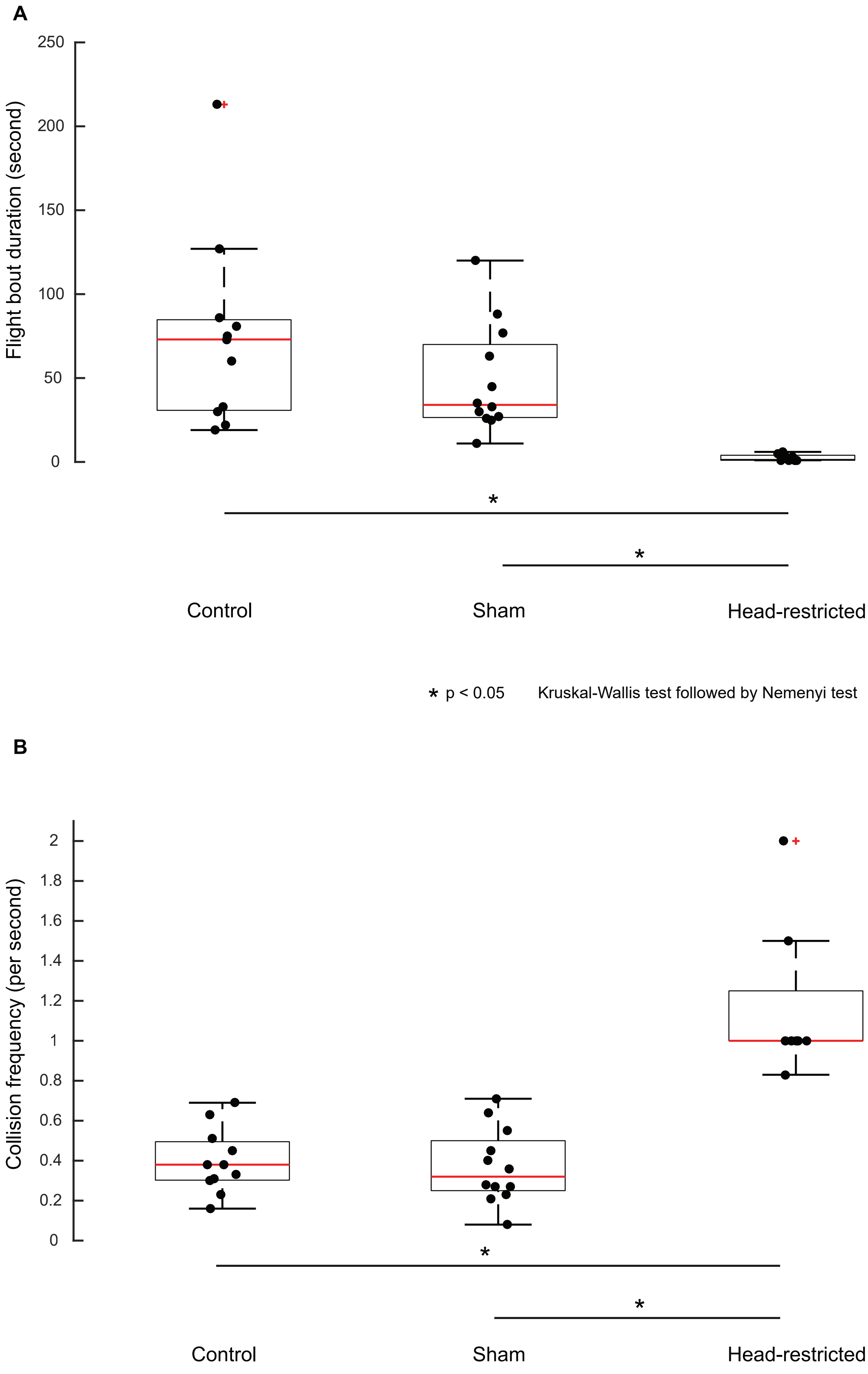
A
Flight bout duration (second)
250
200
150
100
50
0
*
*
Control
Sham
Head-restricted
* p < 0.05
Kruskal-Wallis test followed by Nemenyi test
B
Collision frequency (per second)
2
1.8
1.6
1.4
1.2
1
0.8
0.6
0.4
0.2
0
*
*
Control
Sham
Head-restricted

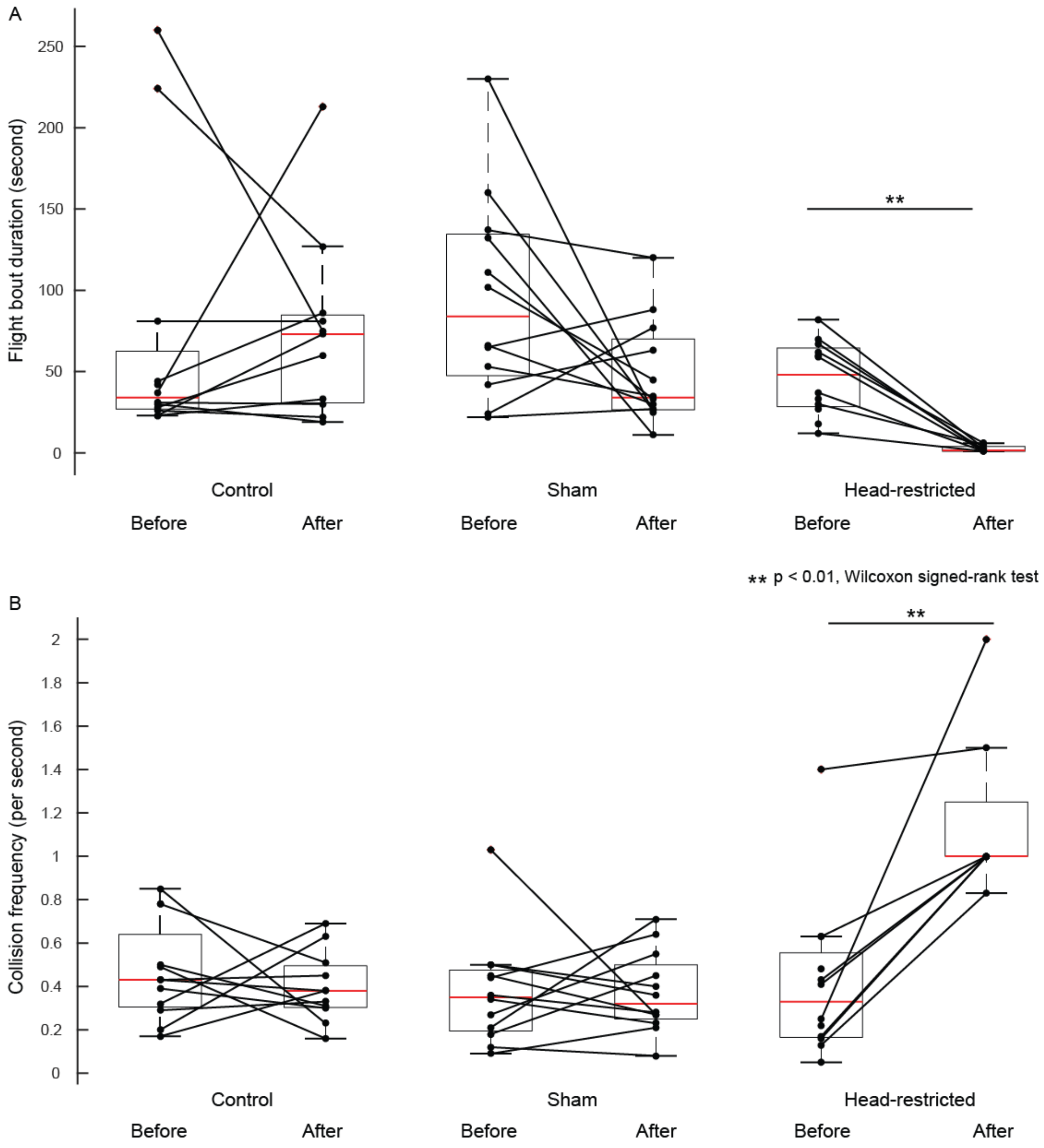

Supplementary Figure 1. Boxplots comparing flight bout duration **(A)** and collision frequency **(B)** of experimental moths with their corresponding pre-treatment conditions (internal control). The flight bout duration and collision frequency of the control and sham moths did not differ significantly from their corresponding pre-treatment conditions ($p > 0.05$, Wilcoxon signed-rank test, pre-treatment: $n = 12$, post-treatment: $n = 11$ (control), $n = 12$ (sham)). Both parameters differed in the head-restricted moths from their pre-treatment conditions. ($p = 0.0078$, Wilcoxon signed-rank test, pre-treatment: $n = 12$, post-treatment: $n = 8$)

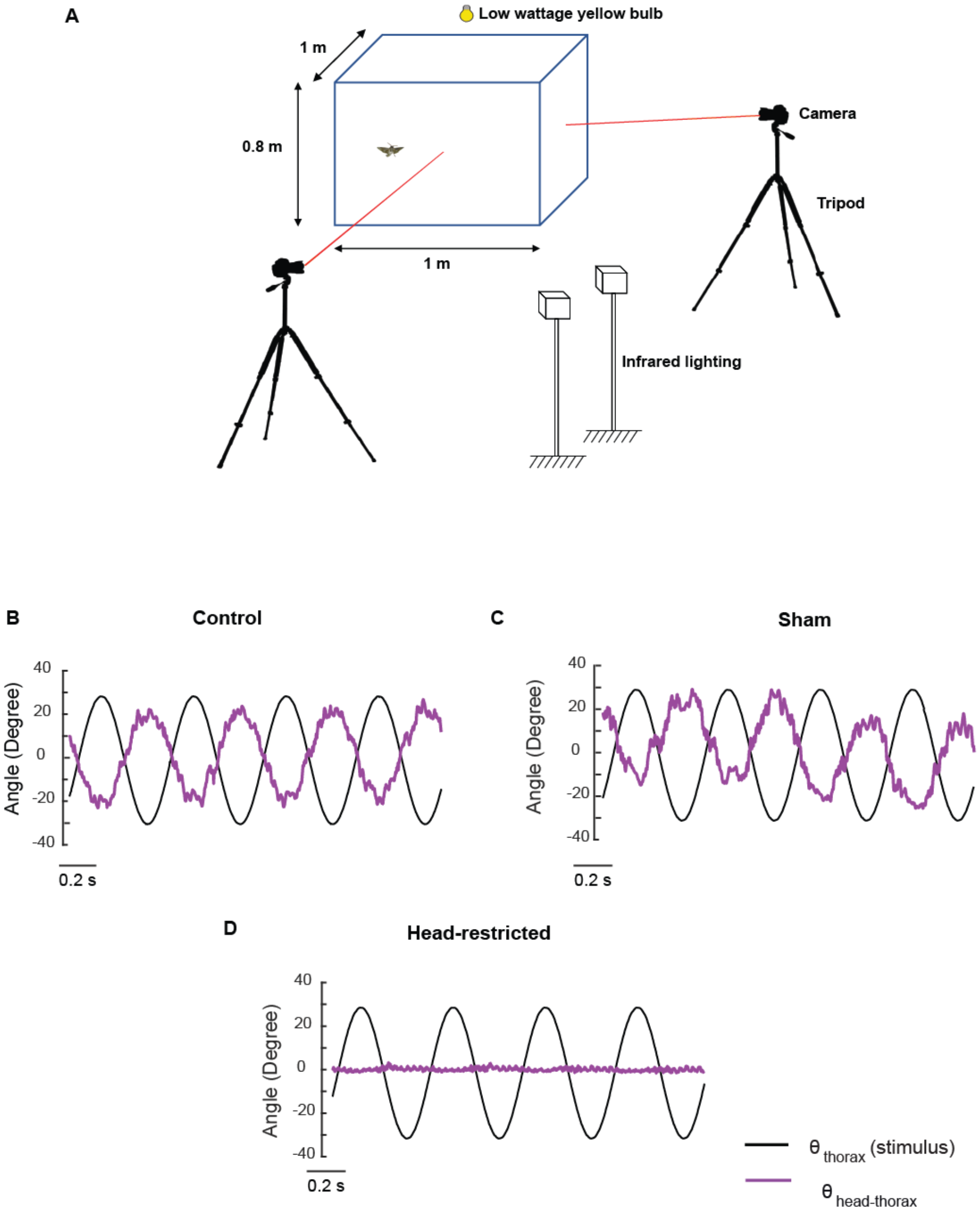

Supplementary Figure 2. A. Diagrammatic representation of the free-flight assay**. (B-D)** Experiments on tethered moths to confirm the presence of head stabilization in the control (B) and sham (C) moths but no head stabilization in the head-restricted (D) case.

.

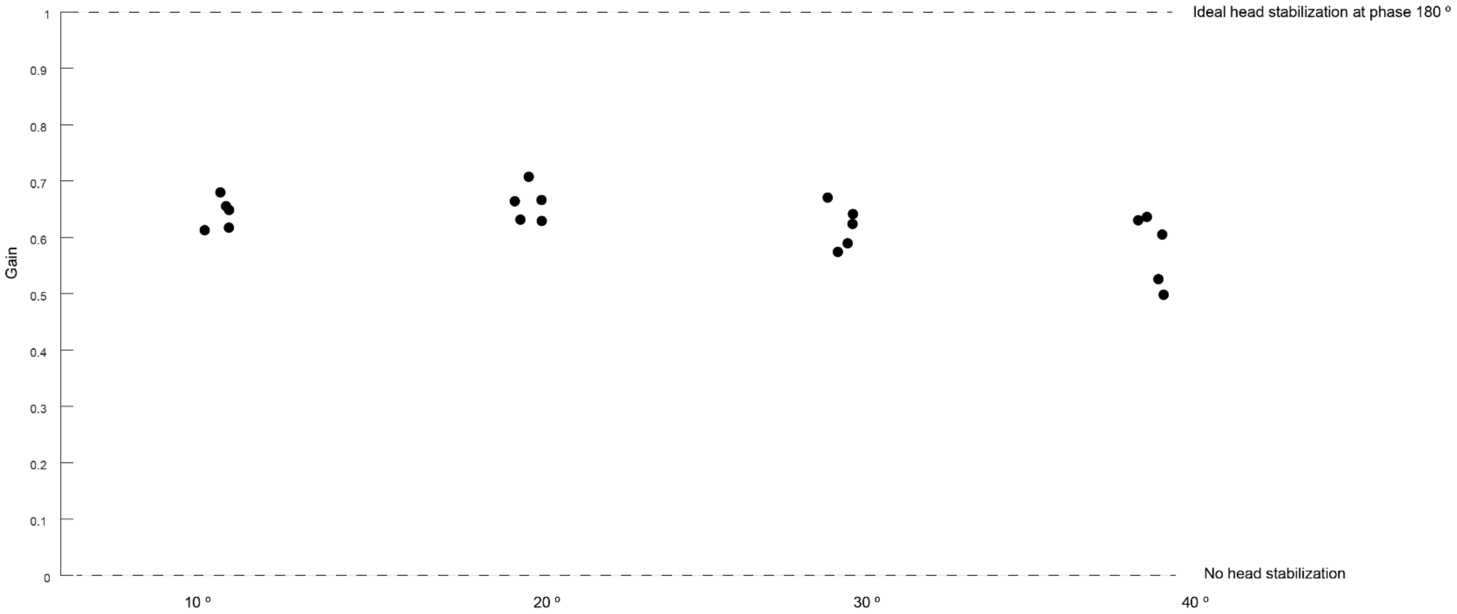

Supplementary Figure 3. Scatterplots of gain at different stimulus amplitudes. The gain does not differ between the different stimulus amplitudes.

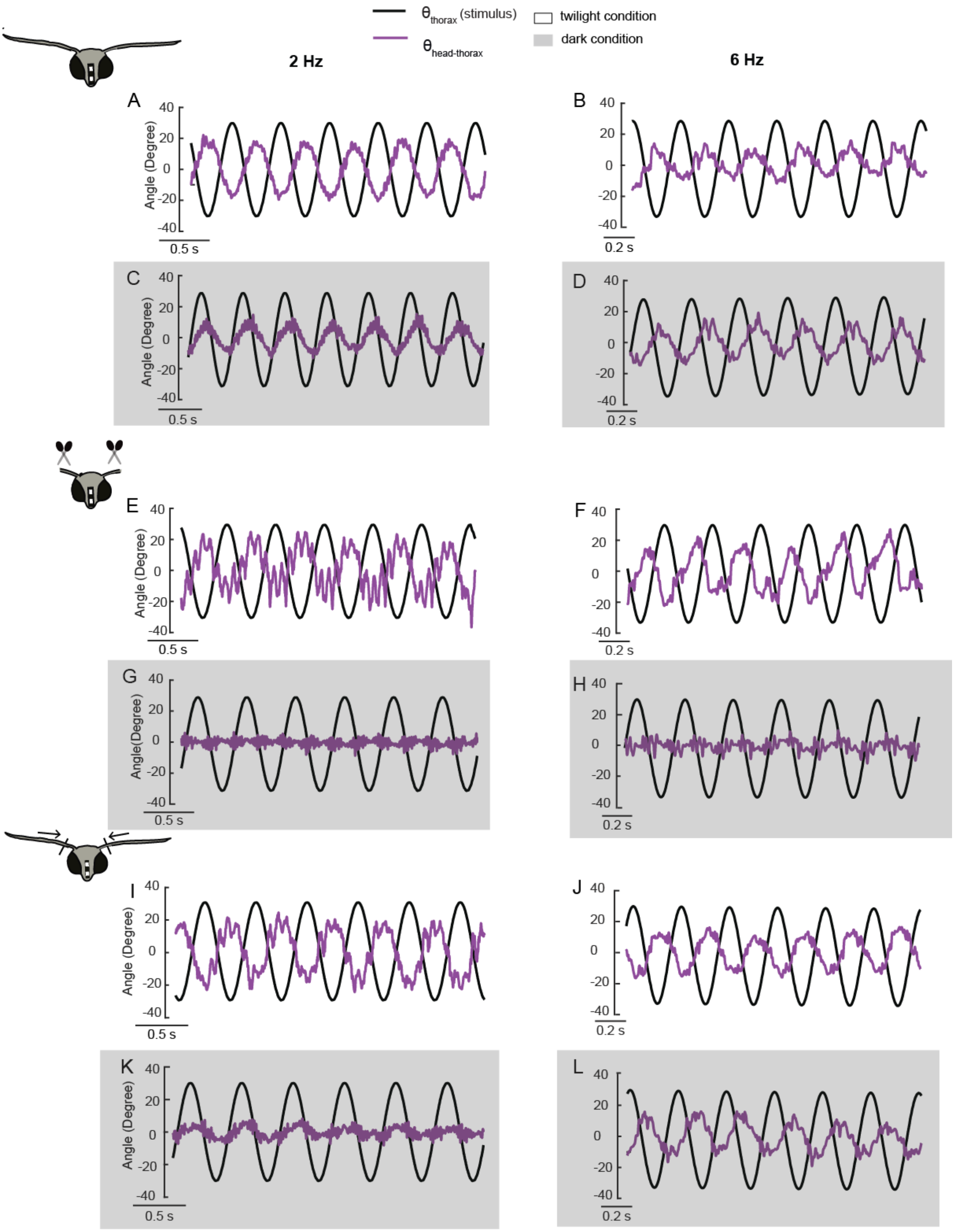

Supplementary Figure 4. Representative time-domain plots in twilight and dark conditions (gray shaded) at 2 Hz (left column) and 6 Hz (right column) in *flagella-intact* (A-D), *flagella-clipped* (E-H) and *flagella-reattached* (I-L) groups.

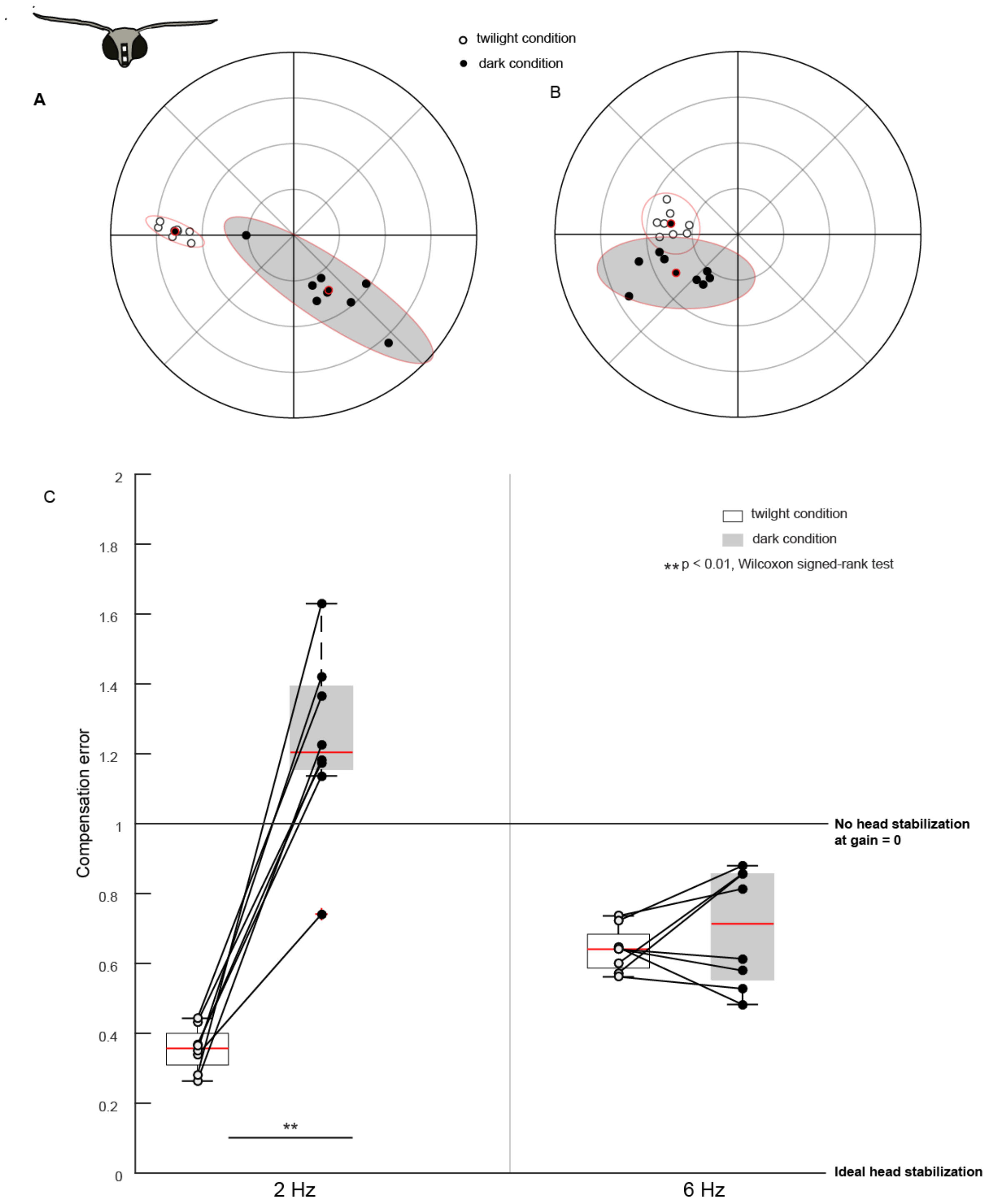

Supplementary Figure 5. Fig. 2 is repeated with an alternative way of phase computation (fourier based phase estimation). The results from Fig. 2 remain unaltered using this way of phase estimation.

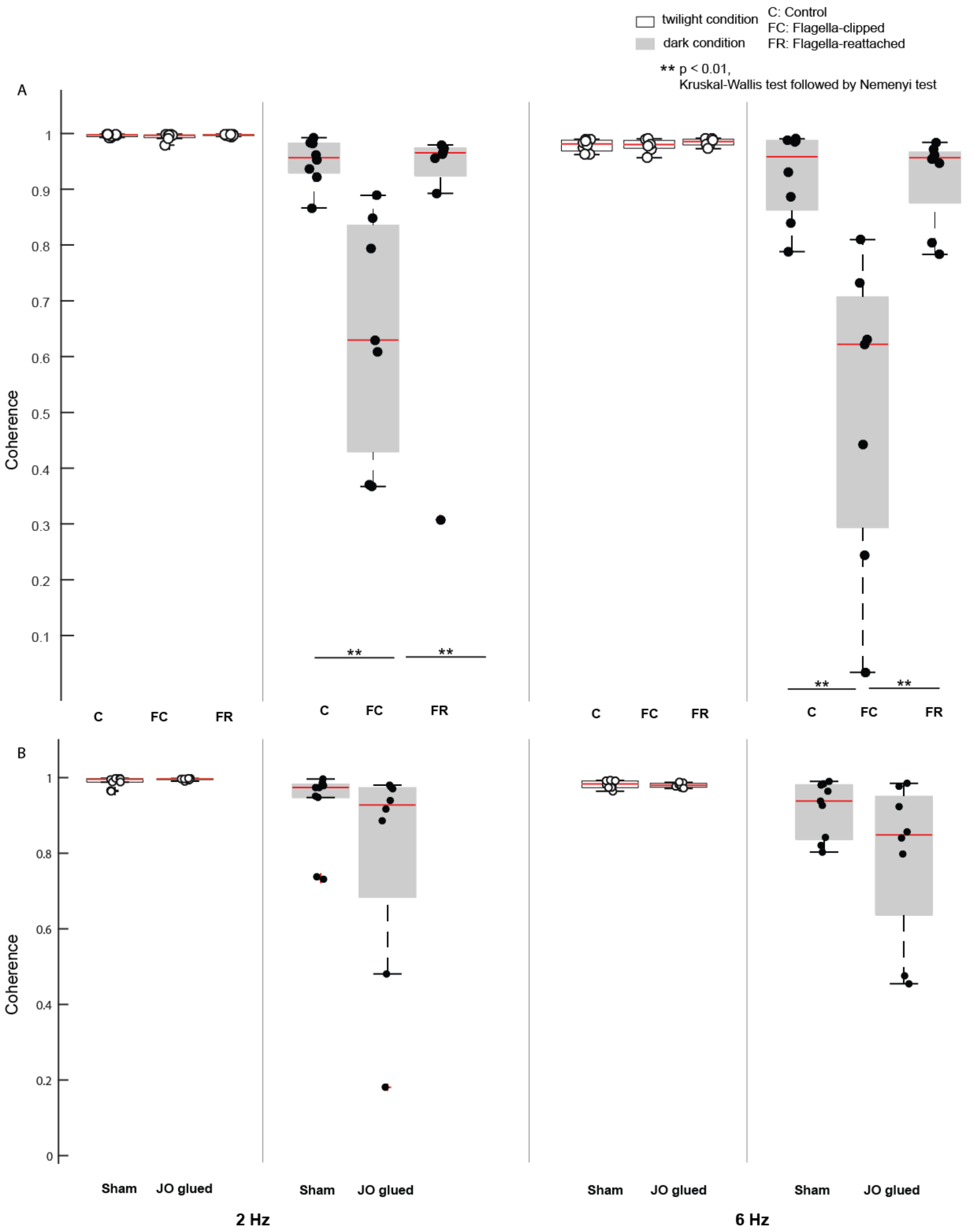

Supplementary Figure 6. A. Boxplots comparing coherence estimates in *control*, *flagella-intact* and *flagella-reattached* groups for twilight and dark trials (shaded boxplots) at 2 Hz (left six boxplots) and 6 Hz (right six boxplots). B. Boxplots comparing coherence estimated in *sham* and *Johnston's organ glued* groups for twilight and dark trials (shaded boxplots) at 2 Hz (left four boxplots) and 6 Hz (right four boxplots).

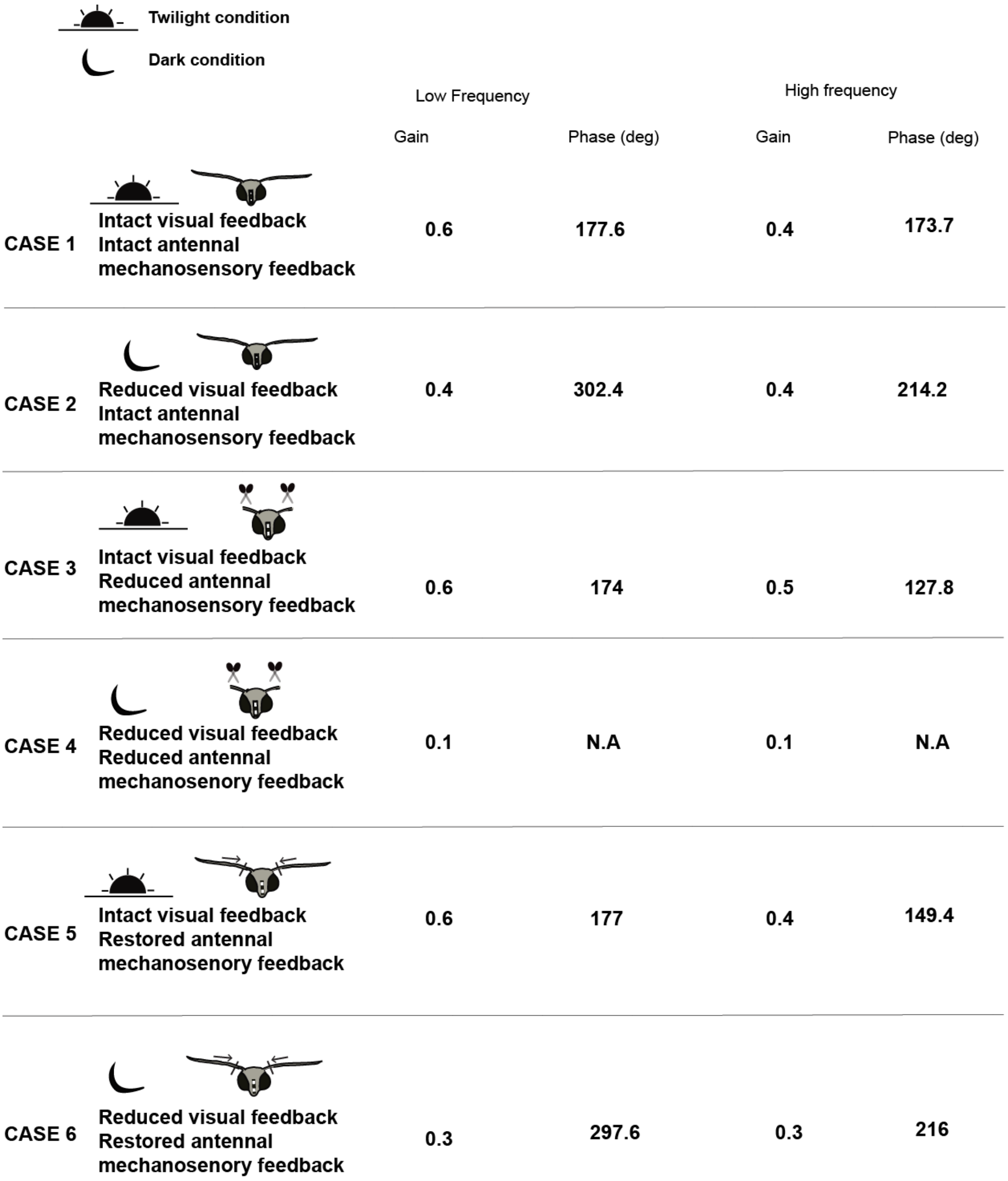

Twilight condition

Dark condition

		Low Frequency		High frequency	
		Gain	Phase (deg)	Gain	Phase (deg)
CASE 1	**Intact visual feedback Intact antennal mechanosensory feedback**	**0.6**	**177.6**	**0.4**	**173.7**
CASE 2	**Reduced visual feedback Intact antennal mechanosensory feedback**	**0.4**	**302.4**	**0.4**	**214.2**
CASE 3	**Intact visual feedback Reduced antennal mechanosensory feedback**	**0.6**	**174**	**0.5**	**127.8**
CASE 4	**Reduced visual feedback Reduced antennal mechanosenory feedback**	**0.1**	**N.A**	**0.1**	**N.A**
CASE 5	**Intact visual feedback Restored antennal mechanosenory feedback**	**0.6**	**177**	**0.4**	**149.4**
CASE 6	**Reduced visual feedback Restored antennal mechanosenory feedback**	**0.3**	**297.6**	**0.3**	**216**

Supplementary Figure 7. List of median values of gain and phase for the different conditions of *flagella-intact*, *flagella-clipped* and *flagella-reattached* moths.

Supplementary methods

Compensation error

Distance between two points p_1 and p_2 with polar coordinates (r_1, θ_1) and (r_2, θ_2) is given by

$$d = \sqrt{r_1^2 + r_2^2 - 2r_1 r_2 \cos(\theta_1 - \theta_2)}$$

Compensation error was computed as the distance between perfect head stabilization point and experimental point. Setting p_1 as the perfect head stabilization point with coordinates (1, 180°), we get the compensation error of the experimental point p with coordinates (r, θ) as

$$\varepsilon = \sqrt{1 + r^2 - 2r\cos(180° - \theta)}$$

$$\varepsilon = \sqrt{1 + r^2 + 2r\cos\theta}$$

Supplementary table

1. List of Interquartile Range of Compensation error

Groups	Twilight_2Hz	Twilight_6Hz	Dark_2Hz	Dark_ 6Hz
Flagella-intact	0.09	0.11	0.22	0.27
Flagella-clipped	0.06	0.13	0.03	0.07
Flagella-reattached	0.08	0.09	0.18	0.08
Sham	0.12	0.1	0.26	0.28
Johnston's organ glued	0.05	0.22	0.18	0.18

2. List of interquartile ranges of Coherence

Groups	Twilight_2Hz	Twilight_6Hz	Dark_2Hz	Dark_ 6Hz
Flagella-intact	0.00	0.02	0.05	0.12
Flagella-clipped	0.01	0.01	0.41	0.41
Flagella-reattached	0.00	0.01	0.05	0.09

Sham	0.01	0.02	0.04	0.14
Johnston's organ glued	0.00	0.01	0.29	0.31

3. Details of the statistical tests used in various experiments in this paper

Groups compared	**n size**	**Tests**	**p-value**	**Groups significantly different (α = 0.05, post-hoc Nemenyi test)**
1.a. Twilight and dark compensation error (***Flagella-intact*, 2 Hz**)	Twilight: n = 8 Dark: n =8	Wilcoxon Signed-rank	0.0078	Not applicable
b. Twilight and dark compensation error (***Flagella-intact*, 6 Hz**)	Twilight: n = 8 Dark: n = 8	Wilcoxon Signed-rank	0.5469	Not applicable
c. ***Flagella-intact, Flagella-clipped and Flagella-reattached*** **compensation error** (**Twilight, 2 Hz**)	Flagella-intact: n=8, Flagella-clipped: n = 7, Flagella-reattached: n = 8	Kruskal-Wallis test followed by Nemenyi test	0.0107	Flagella-intact, flagella-clipped
d. ***Flagella-intact, Flagella-clipped and Flagella-reattached*** **compensation error** (**Dark, 2 Hz**)	Flagella-intact: n=8, Flagella-clipped: n = 7, Flagella-reattached: n = 8	Kruskal-Wallis test followed by Nemenyi test	0.0133	Flagella-intact, flagella-clipped
e. ***Flagella-intact, Flagella-clipped and Flagella-reattached*** **compensation error** (**Twilight, 6 Hz**)	Flagella-intact: n=8, Flagella-clipped: n = 7, Flagella-reattached: n = 8	Kruskal-Wallis test followed by Nemenyi test	0.0064	Flagella-intact, flagella-clipped
f. ***Flagella-intact, Flagella-clipped and Flagella-reattached*** **compensation error** (**Dark, 6 Hz**)	Flagella-intact: n=8, Flagella-clipped: n = 7, Flagella-reattached: n = 8	Kruskal-Wallis test followed by Nemenyi test	0.0011	1. Flagella-intact, flagella-clipped 2. Flagella-clipped, flagella-reattached
g. ***Sham*** **and** ***Johnston's organ glued*** **compensation error (Twilight, 2 Hz)**	Sham: n = 12 Johnston's organ glued: n = 7	Wilcoxon ranksum	0.5358	Not applicable
h. ***Sham*** **and** ***Johnston's organ glued*** **compensation error (Dark, 2 Hz)**	Sham: n = 10 Johnston's organ glued: n = 8	Wilcoxon ranksum	0.0831	Not applicable
i. ***Sham*** **and** ***Johnston's organ glued*** **compensation error (Twilight, 6 Hz)**	Sham: n = 10 Johnston's organ glued: n = 7	Wilcoxon ranksum	0.0097	Not applicable

j. *Sham* and *Johnston's organ glued* compensation error (Dark, 6 Hz)	Sham: n = 9 Johnston's organ glued: n = 8	Wilcoxon ranksum	0.0055	Not applicable
k. Flight bout duration of *Control, sham and Head-restricted moths*	Control: n = 11 Sham: n = 12 Head-restricted: n = 8	Kruskal-Wallis test followed by Nemenyi test	0.0001	1.Control, Head-restricted moths 2. Sham, Head-restricted moths
l. Collision frequency of *Control, sham and Head-restricted moths*	Control: n = 11 Sham: n = 12 Head-restricted: n = 8	Kruskal-Wallis test followed by Nemenyi test	0.0002	1.Control, Head-restricted moths 2. Sham, Head-restricted moths

In the plots below, we have estimated power ie, the probability of detecting a difference between the groups with a significance level of 0.05 across a range of sample sizes for all the comparisons which yielded significant difference. We have used the relevant tests i.e, Wilcoxon signed-rank, Wilcoxon rank-sum and Kruskal-Wallis tests for the power analysis. In all the plots, the power of 0.8 is marked in dotted line. Our sample size in all cases (mentioned below the plots) is greater than or close to the power of 0.8.

1. Fig. 2

Twilight Vs Dark (Frequency: 2 Hz imposed roll)

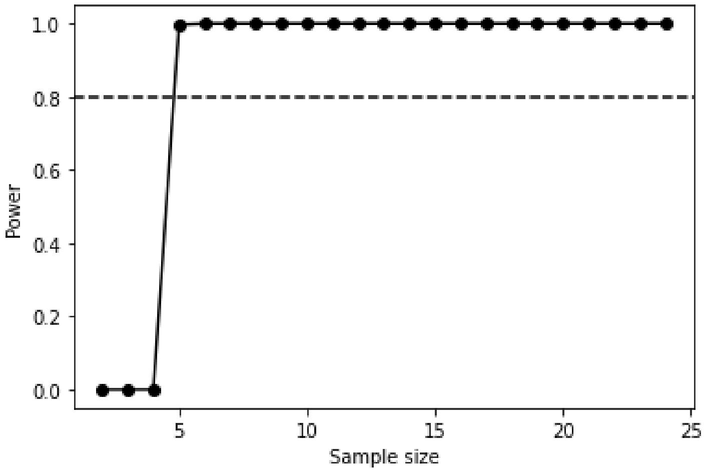

Twilight: n = 8, Dark: n = 8. The minimum sample size required for having a power 0.8 is 5.

2. Fig. 3

Control, Flagella-clipped and Flagella-reattached (Frequency: 2 Hz imposed roll, light level: twilight)

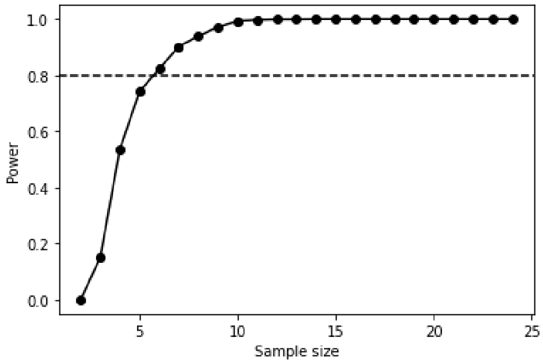

Control: n = 8, Flagella-clipped: n = 7, Flagella-reattached: n = 8. The minimum sample size required for having a power 0.8 is 6.

Control, Flagella-clipped and Flagella-reattached (Frequency: 2 Hz imposed roll, light level: dark)

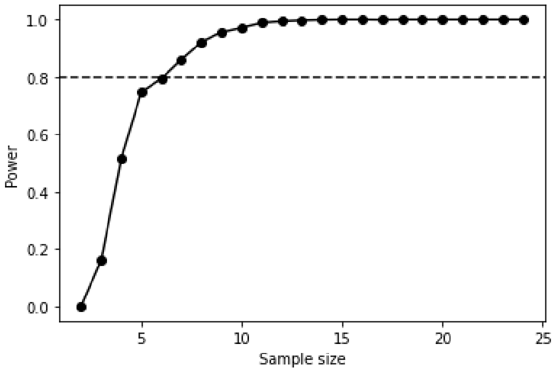

Control: n = 8, Flagella-clipped: n = 7, Flagella-reattached: n = 8. The minimum sample size required for having a power 0.8 is 6.

Control, Flagella-clipped and Flagella-reattached (Frequency: 6 Hz imposed roll, light level: twilight)

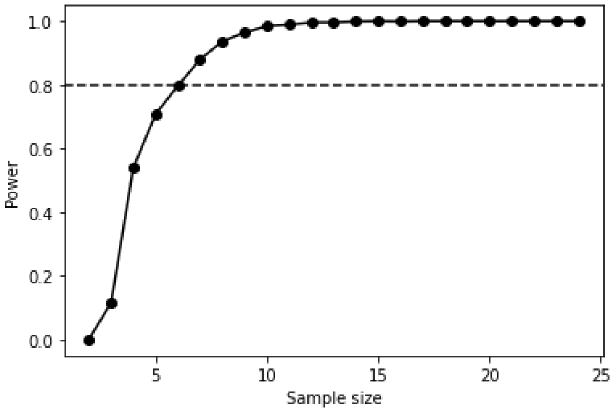

Control: n = 8, Flagella-clipped: n = 7, Flagella-reattached: n = 8. The minimum sample size required for having a power 0.8 is 6.

Control, Flagella-clipped and Flagella-reattached (Frequency: 6 Hz imposed roll, light level: dark)

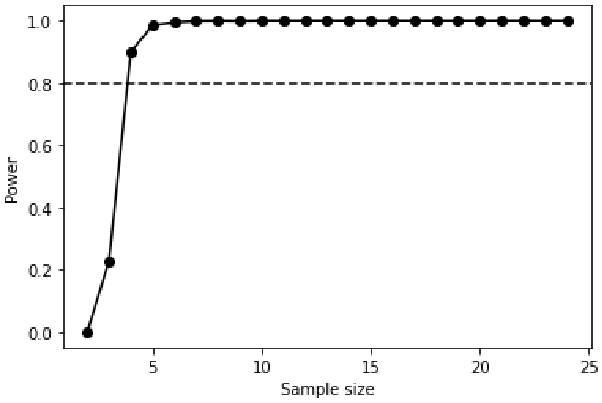

Control: n = 8, Flagella-clipped: n = 7, Flagella-reattached: n = 8. The minimum sample size required for having a power 0.8 is 4.

3. Fig. 4

Sham and Johnston's organ glued (Frequency: 6 Hz imposed roll, light level: twilight)

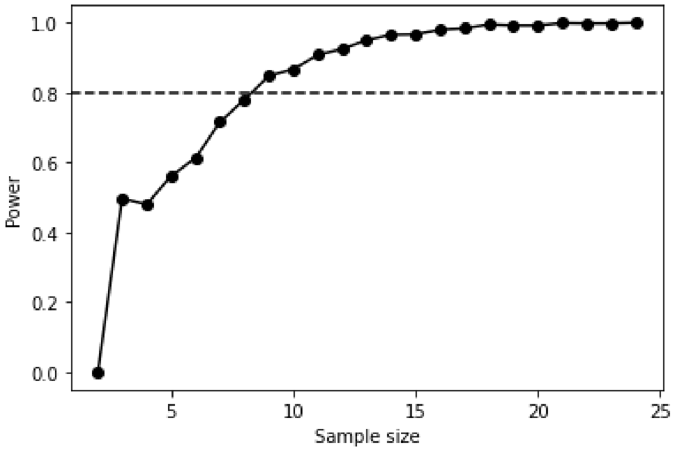

Sham: n = 10, Johnston's organ glued: n = 7. The minimum sample size required for having a power 0.8 is 9.

Sham and Johnston's organ glued (Frequency: 6 Hz imposed roll, light level: dark)

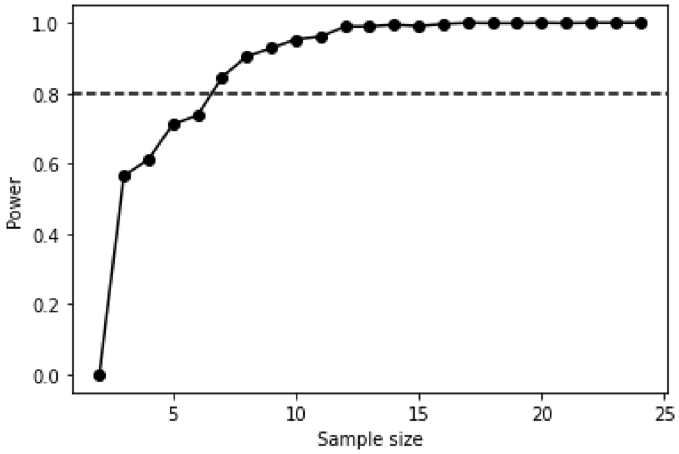

Sham: n = 9, Johnston's organ glued: n = 8. The minimum sample size required for having a power 0.8 is 7.

4. Fig. 6

Control, Sham and Head-restricted (flight bout duration)

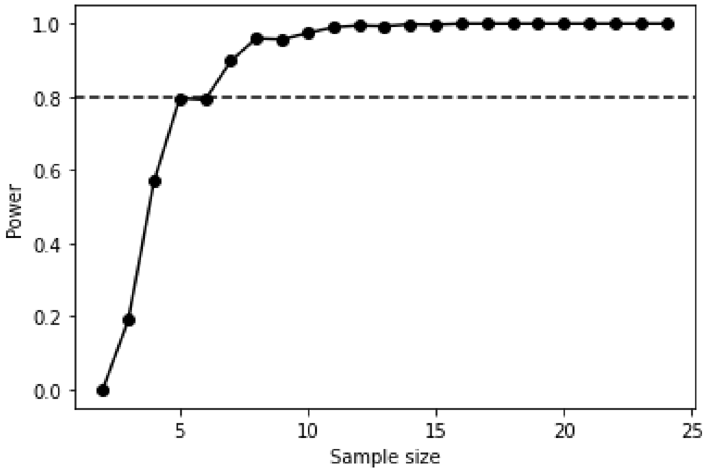

Control: n = 11, Sham: n = 12, Head-restricted: n = 8. The minimum sample size required for having a power 0.8 is 5.

Control, Sham and Head-restricted (Collision frequency)

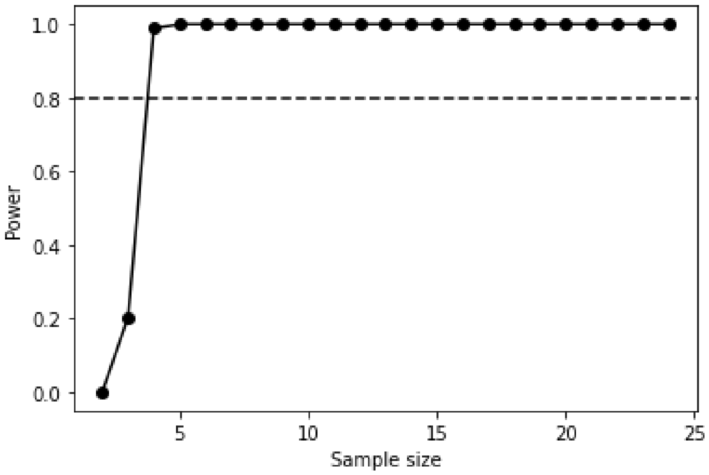

Control: n = 11, Sham: n = 12, Head-restricted: n = 8. The minimum sample size required for having a power 0.8 is 4.